GEM TN-91-30

CONSIDERATIONS LEADING TO THE CHOICE OF OPEN FIELD MAGNET

R. Stroynowski
Southern Methodist University

GEM-TN-91-30
SMUHEP 91-11
November 1991

Considerations Leading to the Choice of Open Field Magnet

R. STROYNOWSKI

Southern Methodist University, Dallas, Texas 75275

1. Executive Summary

1. After reviewing various design options, the GEM Collaboration decided to propose a single coil superconducting solenoid magnet. The decision was based on comparison of physics performance, cost, technical risks and schedule.

2. Conceptual design of a baseline magnet has been completed and found to be feasible and realistic in terms of its performance and cost.

3. The baseline magnet can be further optimized in terms of its size, field and cost. It provides an opportunity for additional improvements of the muon system physics performance in the forward direction by modification of the magnet poles, and in the central region by the addition of muon chambers outside of the unshielded coil.

4. Mitigation of the fringe magnetic field has been investigated in detail and presents no special technical problems. The analysis indicates that the cost of mitigation will not exceed $5M.

5. The proposed magnet has severe procurement and schedule difficulties and will require rapid development of special strategies.

2. General Considerations

The physics motivations of the GEM experiment are well summarized in the Letter of Intent. Briefly, it aims at the search for the production of new, massive particles in the high energy proton-proton collisions available at the SSC. These may be either scalar Higgs bosons expected in the Standard Model of electroweak interactions or some of the many new particles proposed in other theoretical models discussing high energy collisions: supersymmetry, technicolor, leptoquarks etc. The expected signatures of the decays of such new particles are usually high energy photons, leptons emitted at large transverse momentum, or multiple jets of charged and neutral particles. The concept of the GEM experiment is to maximize the probability of discovery of these new particles by

optimizing the capability of the detector to measure high energy photons, electrons and muons while maintaining the possibility of measuring the energy and direction of hadronic jets. This concept leads to the requirements for excellent resolution of the muon momentum measurements and of the electron and photon energy and direction measurements. These in turn, lead to a necessity of minimizing the amount of intervening material in front of the electromagnetic calorimetry and to the necessity of measuring the muon tracks inside the magnetic field. The above criteria are fulfilled by the design of the detector, where a solenoidal magnet with very large radius encompasses muon tracking stations and electromagnetic calorimeter inside the coil.

The technical complexity of building large solenoid coils leads further to the selection of a superconductiong solenoid with moderate field of about 0.8 Tesla. Such field can be achieved well within the "state of the art" technology with a simple, single winding coil. Higher fields would require multilayer winding and would push the magnet building technology towards high risk solutions. Resistive magnet technology was also considered and was found to be impractical. At a field value of about 0.4 Tesla (such as proposed by the L* experiment) the momentum resolution requirements lead to a very large size magnet and large power consumption during the operation estimated at about 20 MW. The resistive magnet requires a large iron return yoke and the associated construction schedule and operational cost is unacceptable. At the same time, such low magnetic field does not provide sufficient bending power for the succesful employment of the inner tracker. The increase of the magnetic field from its low value mandates change to the superconducting technology. Further reduction of the cost may be achieved by the removal of the iron flux return yoke.

This note summarizes the analysis by the physicists involved in the GEM experiment proposal preparation, the GEM magnet design team and the GEM Magnet Technical Review Panel leading to the proposed choice. The supporting notes are listed in the accompanying bibligraphy.

2.1 Magnet design group and GEM Magnet Technical Panel

The magnet design group consists of physicists from the GEM Collaboration and the engineering teams from the Lawrence Livermore National Laboratory, Massachusetts Institute of Technology Plasma Fusion Center and National High Magnetic Field Laboratory (Florida). During the past five months the MIT PFC team of about ten engineers and designers led by Peter Marston and Bruce Montgomery concentrated on the calculations of the shape of the magnetic field for various options of the magnet coil and iron poles, and on the problem of local shielding of the fringe field of the proposed magnet. The LLNL group of eleven engineers and designers led by Gary Deis, Coleman Johnson and Anthony Chargin concentrated on the mechanical design of the magnet and of its "cold mass" structure and on its integration with other detector subsystems and with the experimental hall.

The work of this team has been reviewed by the GEM Magnet Technical Panel convened by the SSC Laboratory. The Panel membership included international experts, as well as representatives of various large industrial companies which built superconducting magnets in the past, eg. General Dynamics, Westinghouse, Ensaldo, and industrial contractors representing conductor suppliers, vacuum vessel manufacturers etc. The Panel worked together with the GEM magnet team in an interactive mode. It met three times to discuss various aspects of the design and produced reports of the meetings. Its recommandations have been incorporated into the proposed magnet design. Several excerpts from the panel reports are given in the following sections.

3. Options

Since the concept of the resistive magnet has been rejected early on, the magnet design group considered three general options:

1) Superconducting solenoid with fringe magnetic field

2) Superconducting solenoid with iron return yoke

3) Double concentric coils superconducting solenoid where the flux generated by one coil is returned by the second coil

The three options were examined from the point of view of cost, construction time and risks involved in the design and construction. All of these were major factors in the final choice of option 1.), which is the only one with acceptable cost, risk and schedule. Below, we list briefly the arguments used to make the selection.

3.1 Cost considerations

The general constraint of the GEM detector design is imposed by the cost guidelines stated by the SSCL Program Advisory Commitee, namely that the overall cost of the detector should be less than $500M. Within this constraint the GEM Collaboration set a goal for the cost of a magnet subsystem and related structures at $120M plus a portion of the R&D funds. This goal represents the only viable compromise between the needs to build a large, reliable magnet fulfilling the criteria imposed by the physics requirements and the costs of other detector subsystems.

The cost of the baseline design consisting of the single coil solenoid with unconstrained field has been worked out in detail by the design group and is presented in the WBS format. This cost, summarised in Table 1, was reviewed by the GEM Magnet Technical Panel and found to be credible.

Table 1: Cost estimate for magnet subcomponents.

	Cost Estimate in $k	Contingency in $k	Contingency in%
Magnet R&D	4871	0	0
Preliminary Design	4903	0	0
Coil assemblies	36446	10255	28
Poles and support	14874	3138	21
Central detector support	4095	983	24
Power/protection	832	136	16
Cryogenics	8680	1418	16
Vacuum	856	97	11
Controls	285	51	18
Installation	6925	1799	26
Management	3552	568	16
Total	86319	18445	21
Grand total		104764	

The cost of possible improvements of the magnetic field in the forward direction leading to better muon momentum measurement is not included in the above table. Modifications of the present design considered so far may introduce additional cost of about $10M.

The cost of the solenoid with iron return yoke includes all costs listed in Table 1 and the additional cost of iron barrel shielding and its installation. In order to limit the fringe field to approximately 1 gauss at the surface above the experimental hall, a 2.0 m thick iron barrel is required around the solenoid. The weight of such barrel was estimated to be about 36,000 tonnes and the cost, excluding installation, was estimated to be $99.0M bringing the total cost of the magnet to about $203M.

A somewhat less expensive partial shielding solution in form of a 1.3 m thick barrel around the solenoid was also considered. It would reduce the stray field at the surface to about 10 gauss level immediately above the detector hall and would require about 20,000 tonnes of iron at an additional cost of $55.5M i.e., a total cost of about $160M. However, the fringe magnetic field in the experimental hall

would remain significant for such partial shielding. Such an option, therefore, does not provide significant advantages over the unshielded solution.

The cost of the double coil solenoid was estimated relative to the cost of the single coil magnet. The second coil, outside of the one costed above, would have a larger coil diameter and larger stored energy. The cost increase for the double coil was made using the following factors:

1) Ratio of stored energy = 2.3

2) Amp turn ratio = 3.2

3) Coil diameter ratio = 1.3

For the items not related to these factors, the cost increase was based on engineering judgment. The overall cost increase for the double coil solution was estimated to be of the order of $100M over the cost of a single coil magnet bringing the total to over $200M.

In summary options 2.) and 3.) were estimated at about twice the cost of option 1.).

3.2 Construction Time

In a typical high energy physics experiment, delays in construction of a sub-component can be significant, but usually can be partially offset by speeding up a construction of other components. Such is not a case of the proposed GEM detector. Here, any delay of the magnet construction translates linearly not only into the delay of the completion date of the overall experiment, but also impacts the completion and testing of the main ring of the SSC accelerator. It should be emphasised that the present construction schedule already represents a major problem since it requires initiation of procurements of major componenets before the Technical Design Report will be finalized.

The construction schedule of the single coil magnet was designed to fulfill the requirement of completion of the detector installation at the time when SSC

ring has to be closed for beam testing. This schedule illustrated in Fig.1 requires completed and tested magnet to be available in the underground experimental hall in April 1997 in order to allow for installation of the rest of the detector.

The milestones of the construction are defined by the estimate of 12 months needed for the conductor manufacturing process, 14 months for the winding of the coil sections and 6 months for the assembly and testing. These milestones rely on a Beneficial Occupancy Date of the magnet construction surface facilities in 1993 and on a Beneficial Occupancy Date of the underground hall in 1995. Furthermore a number of procurement decisions will have to be made in summer of 1992.

The proposed schedule calls for magnet construction using two shifts a day and a large number of components prefabricated off-site. The schedule was reviewed by the GEM Magnet Technical Panel and was found to be tight, but possible, provided that agressive R&D is pursued in the FY92 and that an early and effective procurement strategy is developed. The panel suggested several time saving procedures included in the present scenario which include, among others, a recommendation that the magnet tests should not be done at the surface but only after completion of its assembly in the experimental hall.

The time schedule of the iron shielded coil is longer due to assembly time of the iron shield. The additional time needed to lower the iron into the underground hall and to assemble it around the magnet coil was estimated to be from 3.5 to 6 months depending on whether the experimental hall will have one or two access shafts with independent cranes.

The impact of the double coil option on the schedule is somewhat more difficult to estimate. Assuming that the coil manufacturing process could be parallelized by creating independent winding stations for the outside coil, the main impact would be the extension of the construction schedule by about 3 months due to increased complexity of installation.

In summary, the magnet construction time represents a major tactical issue for the GEM experiment. Only option 1.) schedule can be fitted (with difficulties) into the overall SSC accelerator time table.

3.3 Technical risks

The base line option of the single coil magnet represents a conservative design with a low estimated risk with regard to technical feasibility. The distinctive features of the magnet are its very large size and stored energy and a large operating current. Although the size is about three times larger that that of magnets of present generation of high energy physics experiments, the field is substantially lower. The stored energy and operating current are comparable to that of large scale magnetic confinement fusion devices built in the past decade. The large size primarily affects manufacturing, transportation and installation. It is believed that these factors do not adversely affect feasibility.

The iron shielded option of the magnet presents also a low technical risk. The technical problems of the coil are basically the same as that of the unshielded option and the mechanical support for the additional iron represents a solvable engineering problem. It should be noted, however, that the reduced space available in the experimental hall and the substantial load on the hall floor represents added complexity to the experimental facilities.

The double coil concept of the magnet presents significant technological risks. The two coils must be supported in such a way as to prevent mechanical instabilities due to the substantial forces between them. The two coils would also require different windings schemes introducing a necessity of development of additional tooling. The total length of the conductor in the two coils would increase by about a factor of four with respect to the single coil solution increasing the probability of winding and cryogenics problems occuring during the manufacturing process.

3.4 Financial and technical conclusions

A comparison of the relative costs of the three magnet options discussed, shows that the magnet shielded either by iron or by a second coil costs about $100M more than the unshielded option. The cost of mitigation of the effects of the fringe magnetic field is estimated at less than $5M (see chapter 6). In addition the increased complexity of the construction and assembly of the iron shield or of a second coil poses substantial risks of delays and difficult technical problems. Thus from the technical and financial point of view the unshielded magnet represents a preferred option.

In the following sections, the consequences of choosing such options are examined.

4. Basic parameters of proposed GEM magnet

The conceptual design of the magnet is almost complete, although its dimensions and field have not yet been optimized with respect to cost and physics performance. The design of the iron poles is also not yet complete. Work on the reduction of the weight of the poles and further modifications related to improvement of field in the forward direction continues.

The schematic drawing of the proposed magnet is shown in Fig.2. The operational parameters of the proposed magnet are listed in Table 2.

Table 2: Major Parameters List

Central induction	0.80	T
Mean radius of windings	8.9	m
Outer radius of outer cryostat vessel	9.45	m
Inner radius of inner cryostat vessel	8.40	m
Coil length, end-to-end (per half)	14.44	m
Cryostat vessel length	30.0	m
Conductor length (total)	24	km
Number of turns	408	
Total mass of coil windings (per half)	238	t
Total mass of cryostat vessel (each half)	717	t
Total mass of iron end pole (each)	2950	t
Radial pressure on windings	255	kPa
Inductance	1.47	H
Stored energy	2.04	GJ
Operating current	52.5	kA
Number of ribs per coil assembly	3	
Central membrane maximum z	0.025	m
Winding minimum z	0.25	m
Axial force on poles	63.5e6	N
Axial force on conductor	27.9e6	N
Magnet axis height above hall floor	13.0	m

The corresponding lines of constant magnetic flux are illustrated in Fig.3. Details of the iron poles design have not been finalized at this stage. The modification of the iron poles will change the distribution of the magnetic flux near the poles.

The magnet will be constructed from two independent sets of single layer windings each 14.4 m long. The coil will be wound on the inner side of the 5 cm thick bobbin. The bobbin will be constructed in 24 separate cylindrical sections, 1.2 m long each. Each section will be wound separately and will require only a single length of superconductor. This approach is employed to maximize the reliability of the coil by minimizing the number of conductor splices. The fabrication of the coil in 1.2 m sections allows for winding several sections in parallel thus saving construction time. The winding will be surrounded by a liquid nitrogen radiation shield. The coil assemblies will be supported within the vacuum vessel

by titanium rods connecting to both the 4K coil assembly at one end and to the ambient temperature vacuum vessel at the other end. Support against gravity will be provided by a system of 16 rods oriented roughly tangentially to the bobbin and connected to each end of the bobbin. Support against the axial Lorentz force on the coil will be provided by a set of 16 axially oriented rods providing a tensile preload and preventing any buckling problems. Overall mechanical support will be provided by the stiffened ends of the cryostat vessel. In addition the mechanical structure will have a central support membrane sandwiched between the two halves. The membrane will provide structural support for the coil and the cryostat as well as for the muon chambers and a tube containing calorimeters and the central tracker.

The coil will be surrounded by a liquid nitrogen cooled thermal shield consisting of large aluminium cylinders with serpentine tubes welded on the outside. Details of the assembly are illustrated in Fig.4. The thermal shield will be enclosed in a vacuum vessel constructed from stainless steel for the inner vessel and from low carbon steel for the outer vessel. The outer vessel will incorporate radial and axial stiffeners designed to support the vacuum load and the magnetic load from the poles and the coil.

The cooling for the magnet coil will be obtained by natural convection flow provided by the thermal syphon method. Tubing attached to the outside of the coil bobbin will be connected to headers on the top and bottom to promote free convection. The system can handle all heat loads including thermal radiation, cold mass support conduction and heating in the area of conductor joints. A separate low-flow loop will provide liquid helium to the conductor itself, but this helium will be used only for stabilization, not for cooling. The refrigeration system will be patterned on that of the SSC accelerator.

There are several proposed conductor designs. All of them include standard niobium-titanium conductor with either copper or aluminium stabilizer. The designs differ in the liquid helium cooling arrangements ranging from passive to

forced flow scheme. The choice of the conductor will be made based on its stability and the manufacturing scheme. A high priority R&D program of conductor development and test will be initiated in the next few months. The design and costing is based at present on a high stability "cable-in-conduit" conductor with copper stabilizer.

The base line design also provides an opportunity for further improvements of the muon momentum resolution by placing an additional set of muon chambers 3 m outside the barrel of the magnet. The improvement due to the addditional measurement points and a vertex constraint with 200 μ resolution is illustrated in Fig.5. A distinctive feature of this magnet, apart of its size, is a substantial fringe magnetic field expected both in the experimental hall and on the earth surface. The strength of such fringe field in the undeground area will vary from about 2000 gauss in the vicinity of the magnet poles to about 50-100 gauss in the access shafts. The field strength at the surface will peak at about 40 gauss immediately above the experimental hall and the perimeter of about 10 gauss may extend over the area of about 120 by 180 m. The strength and shape of this fringe field depends very little on the details of the pole design. The field strength contour maps are shown in Figs. 6 and 7.

5. Operational considerations for working with open field magnet

The principal problems related to the stray magnetic field are associated with safety, enviromental issues and experiment operations.

5.1 Health, safety and regulatory aspects of the open field magnet

At present, there are no comprehensive regulatory restrictions of the exposure to magnetic field. Several state, national and international agencies have issued guidelines for magnetic field exposures. These are compiled in the GEM note TN-91-19 and can be summarized as follows:

1. Workers must never be exposed to fields in excess of 2 Tesla regardless of duration of exposure.

2. For fields exceeding 0.5 Tesla, the daily maximum average field strength should not exceed 600 gauss (measured at the torso) or 6,000 gauss measured at the extremities). That translates to a maximum of about 100 minutes full body daily exposure to the full field of GEM magnet.

3. For fields smaller than 0.5 Tesla, the above limits refer to weekly exposures. Thus for a 1000 gauss fringe field the limitation of the full body exposure limits workers to seven eight hours shifts per week.

4. Persons with medical electronic implants (such as eg., cardiac pacemakers) or metallic prostheses should not be exposed to fields in excess of 10 gauss. Persons with sickle-cell anemia or similar hemoglobin-related conditions should not be exposed to fields in excess of 500 gauss.

Thus, the unshielded GEM magnet can operate within all known regulations provided that the access to the areas affected by the stray field is restricted. Access to the areas of the experimental hall where racks of electronics and power supplies will be situated will be accessible to trained personnel with the magnet on.

5.2 Experience in other facilities with unconstrained magnetic filed

There are ample examples of large facilities operating with open field magnets in the United States. The most commonly encountered are the Magnetic Resonance Imaging (MRI) devices in many major hospitals. Many of those have large, unconstrained magnetic fringe field extending over ocupied areas of the hospital buildings. Operational experience can be also obtained from several magnetic confinement fusion and MHD research facilities eg., HFTF, MFTF and FENIX at Lawrence Livermore National Laboratory, ALCATOR C-MOD at the

MIT Francis Bitter Magnet Laboratory and LCT(ISMTF) at Oak Ridge National Laboratory. Finally, the 15-ft Bubble Chamber at Fermilab operated with substantial fringe magnetic field. A comparison of the extent of the GEM magnet fringe field on the earth surface with those of other facilities is shown in Fig.8.

All of the facilities operating with stray field have special operating procedures restricting access to the areas affected to selected and trained personnel. General operating procedures are similar to those applied to the 15-ft Bubble Chamber in Fermilab. These involve search of the affected area for loose ferromagnetic objects before switching on the field, qualification of the lighting, sensory and electrical equipment for operations in the magnetic field, and shielding of sensitive components. In addition the magnets have emergency fast discharge procedures allowing for rapid reduction of the magnetic field. All of the problems encountered are of the "nuisance" type and are readily solvable.

As an example, the field strength contour lines of the MFTF-B facility at LLNL are shown in Fig.9. The field within the experimental hall, indicated by a double solid line, was greater then 100 gauss and exceeded 500 gauss in the vicinity of the magnet. The facility had all the usual valves and electric and electronic equipment operational within the hall, including control and monitoring equipment, high voltage power supplies and various sensors. Similarly, the experience at the FENIX facility indicates that CAMAC and NIM crates and computers including disk drives operate well in the 50 gauss field. The video monitors need, however, to be shielded. Most of other special protection design aspects of the magnetic confinement fusion or MHD devices aim at the effects of rapidly changing fields. Thus, items such as cable trays with gaps between the segments, load bearing I-beams isolated with RG10 sleeves and not-continuous shielding plates will not be necessary in the case of the GEM magnet.

5.3 Effects of stray field on the GEM componenets and operating procedures

In response to the concerns about the forces on ferromagnetic objects, calculations of fringe field dipole-dipole interactions have been done at all points of experimental hall. They are summarized in the note MIT-GEM-EM-01. Briefly, all objects made from magnetically permeable material and located near the detector can experience a force due to the interaction with the field and its local gradient. These forces, illustrated in Fig.10, appear to be rather small. They vary from 0.1 to about 2.5 g in the regions of the crane rails and structural components of the hall. For the structural components of the hall these forces will be a small fraction of the total load carrying requirements. The contours of constant body force are shown in Fig.11. Most of the experimental hall volume has contours values below 1 g. The exception is the area close to the magnet poles where control of loose ferromagnetic objects will be necessary. Forces on the crane will tend to pull it along the rail towards the poles and operation of the crane with the magnet on will not be possible. Design of a locking system for the crane in a parked position appears to have a simple solution. The lighting, electrical and cryogenics equipment will have to be certified for operation in magnetic field. Experience at LLNL and at Fermilab shows that in most cases simple alignment of the equipment along the lines of magnetic field assures its proper operation. This applies to most of the pumps and electrical components using solenoids, as well as to the lighting equipment and vacuum pumps. In cases, where geometrical alignment is not possible, most electrical equipment can be either shielded or oversized to compensate for saturation losses. The availability of standard equipment has been demonstrated at LLNL, where a number of components varying from vaccum pumps and power supplies to electrical interlocks are operational in fields from 50 to 1000 gauss.

During normal operating conditions, access to the experimental hall will be restricted not only due to the fringe magnetic field, but mainly due to the ionizing

radiation generated by the SSC beams. Personnel Access and Safety System being designed by the SSC Laboratory will include the magnet-on condition for the restricted access. The access to the lower counting house may be, however, required while the magnet will be on. Present plan locates the lower counting house in the area of a 50-100 gauss field. The plan also requires the counting house to be shielded.

The general approach to making preparations for energizing the magnet will be through a thorough search-and-secure process before turning the magnet on. The procedure will require the removal of all loose tools and ferromagnetic objects from the vicinity of the iron poles, securing of the necessary equipment like gas bottles, carts etc., and removal of personnel. Such practices are put successfully into operation at FENIX facility at LLNL, L3 experiment at CERN and others.

Normal charge and discharge time of the GEM magnet is limited by the size of the power supplies and by the allowable eddy current heat load to the coil form. As a specific design constraint, the magnet design team set a goal of 300 s for the emergency discharge time in case a rapid access to the experimental hall would become necessary.

6. Special shielding requirements

6.1 Field at the surface

Although there are no regulatory restrictions on the fringe magnetic field on the earth surface, the SSC Laboratory Enviromental Impact Statement states that there will be no measurable magnetic field at the surface of the laboratory. If such statement can be modified, then the access to the area with field exceeding 10 gauss can be controlled by appropriately marked fence and the fact that the field over 1 gauss extends vertically up to about few hundred meters above ground level would require simple notification of the Federal Aviation Administration of the existance of such anomally.

A backup shielding solution is described in note MIT-GEM-EM-02. It consists of an iron plate, possibly a reinforced concrete pad of about 120 x 100 m, with equivalent of about 15 cm of iron in the central region and a lip pointing down at the edges. The estimated weight of iron needed to shield the surface field was estimated to be about 16,800 tonnes. In contrast to the iron needed for construction of return yoke of the magnet, this iron need not be machined and can be quite inexpensive (about $150 per ton). Thus the additional cost of shielding the surface is estimated to be about $3M. Further reduction of the cost of such a surface shield became possible with the change of the interaction hall construction technique from caverning to cut and cover. Here, large part of the surface iron plate can be incorporated into the roof over the experiemntal hall.

6.2 Field in the experimental hall

As described before, the special requirements posed by the presence of the stray field on the equipment in the experimental hall appear to be small. In order to quantify the effects, the estimates of incremental cost of shielding or oversizeing of electrical and cryogenic equipment in the hall were made by Warren Kampmeier. The analysis assumed that for switch-gear and panel boards the breaker sizes would need to be increased by 20% with the corresponding increase of the wire size and cost. Transformers were priced to incorporate cast iron core construction and shielding. Double shielded enclosures were added to electrical motors and added cost was added to include remote mounting of high energy discharge lamp ballast transformers. The overall added cost was estimated to be $55k. Similarly, the added cost for shielding of the cryogenic equipment was estimated at approxiamtely $20k.

Since the magnetic fringe field may affect various electronics and monitoring components, a calculation was done of the requirements and cost of shielding of the lower counting house. It is described in the note MIT-GEM-EM-02. Briefly, shielding of a volume of 20 x 20 x 4 m in an uniform flux density of 50 gauss down to the level of 5 gauss will require 338 tons of iron at a cost of about $300-500k.

Finally, the fringe field of the GEM magnet may affect the final focus magnets of the accelerator. The dominant axisymmetric component of the field will be of the order of 10 to 50 gauss in the vicinity of the low beta quadrupoles. The asymmetric components of the field caused by the magnetic elements in the detector hall eg., structural beams, reinforcement bars and crane rails apear to be small. Because the accelerator low beta quads are encased in steel, little additional shielding may be necessary. Any residual effect will be corrected by using small correction coils around the beam pipe.

6.3 Cost of special shielding

The overall cost of the special shielding will be less then $5M. The components of this estimate are listed in Table 3.

Table 3: Cost of special shielding

	Cost in $
Lower counting house	500,000
Electrical equipment	55,000
Cryogenic equipment	20,000
Surface plate	3,000,000
Contingency	1,000,000
Total	4,575,000

The above cost would remain the same if future the safety and health regulations would become more restrictive by a factor of eg.,ten. The surface plate shield will provide sufficient protection of personnel and of the above ground control room. The lower counting house will be also shielded. Stronger safety rules would result in more restricted access to the unshielded areas of experimental hall and may require strict discipline of access policy enforced by the collaboration. The safety training will become a part of overall safety training procedure required for all personnel. The life cycle cost of operating the experiment under such conditions is being investigated. The issues under study are: possible extended time of an access for safe-and-secure sweep of affected areas, replacement

rate of equipment, training cost and cost of additional maintenance. So far no significant additional cost has been identified.

7. Engineering and R&D program for FY92

There is a number of unresolved conceptual design issues which need to be studied in the next few months. These issues include detailed design of the magnet poles, modifications of the poles leading to the improvement of the momentum resolution in the forward direction, studies of the requirements on the magnet assembly imposed by the needs to preserve the option of adding muon chambers outside of the magnet coil. In addition, the magnet conceptual design has to undergo the optimization process of size vs cost vs field. Finally, the concept of the overall assembly of the magnet has to be examined from the point of view of access to various detector subsystems and overall assembly strategy. Further calculations of the magnetic forces on the magnet and all ferromagnetic objects in the experimentall hall, access shafts and on the surface will have to be made as soon as the shape and location of these objects will become available. These calculations will be particularly important as the design of the experimental hall and associated structures will be firmed up. In addition preliminary design and specifications required for mechanical supports, cryogenics liquid nitrogen and liquid helium systems, power supplies and control and monitoring systems have to be made. All of these issues have to be resolved before the date of the Technical Design Report is due.

The critical path items on the magnet construction schedule are the conductor design and the condutor manufacturing and winding tooling. These items are part of the FY92 R&D proposal to define the conductor and its stabilizer and coil winding procedure and the corresponding tooling. The plan is to develop working relations with industry to produce sample length of the proposed conductor and then test the performance of such sample. The program also includes study to define the acceptable methods of fabrication of 24 km of the conductor.

In addition, a technique for making conductor joints has to be developed and verified.

8. Conclusions

Among all options discussed as candidates for the GEM magnet, the single superconducting coil can be built with lowest cost and risk factors and in shortest time. The shielded magnet versions either by iron yoke or by second external coil cost about $100M more than the unshielded option. The cost of mitigating the effects of the fringe field is estimated to be below $5M. Therefore, the GEM collaboration considers the unshielded magnet option to be the only realistic one within the guidelines of the overall detector cost and schedule.

9. Bibliography

1. GEM Magnet Options, preliminary report. MIT PFC/RR-91-15.

2. GEM Magnet Subsytem, Conceptual Design Cost Estimate. WBS structure prepared by the Lawrence Livermore National Laboratory and MIT Plasma Fusion Center.

3. GEM Magnet Technical Panel reports.

4. R. D. Pillsbury, Fringe Field Dipole-dipole Force Interactions, MIT PFC report MIT-GEM-EM-01.

5. R. D. Pillsbury, L. Myatt and J. Sullivan, Shielding of the Magnetic Fields from the GEM Magnet. MIT PFC report MIT-GEM-EM-02.

6. R. P. Wooley, SSC GEM Magnetic Field Safety & Health Effects, GEM TN-91-19.

7. Warren Kampmeier. SSCL Momoranda on incremental cost of shielding of electrical and cryogenic equipment in the experimental hall.

8. Working in magnetic field. Health and Safety manual, Lawrence Livermore National Laboratory supplement 26.12, June 1985.

9. M. Chaplin and S. Shen. Operational impact of Fringe Magnetic field in FENIX. LLNL Memo.

10. List of figures

1. Schedule of detector and magnet construction.

2. Schematic draing of the GEM magnet.

3. Lines of constant flux for the GEM magnet.

4. Details of the thermal shield assembly around the coil.

5. The improvement of the momentum resolution by the addition of external muon chambers and of the vertex constraint.

6. Fringe field strength contour lines.

7. Surface fringe field contour lines.

8. Comparison of the extent of the GEM magnet fringe field with that of other facilities.

9. Fringe field strength contour lines for MFTF-B facility at LLNL.

10. Magnetic forces in the detector hall.

11. Contours of constant body force in the detector hall.

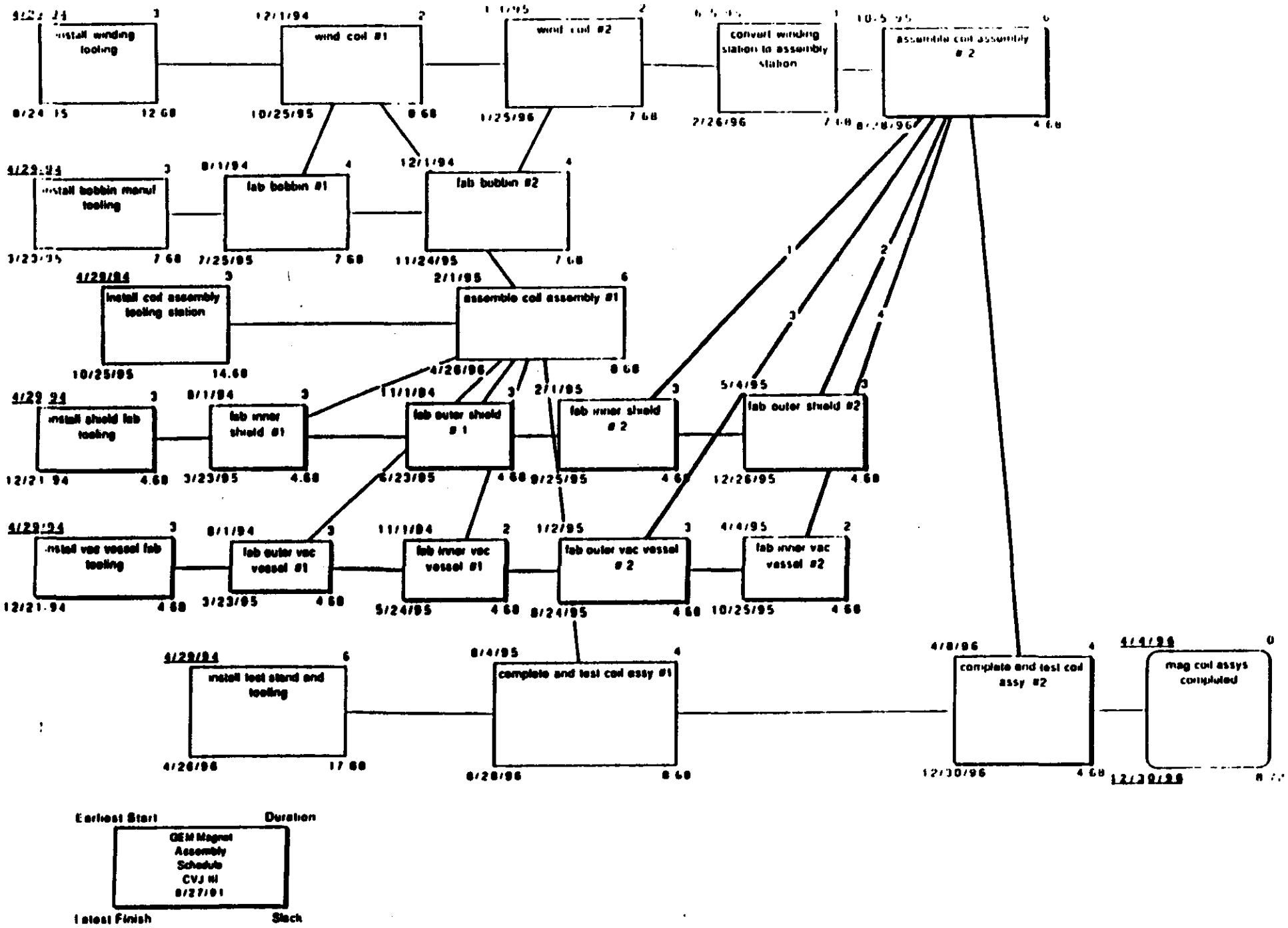
install winding tooling
wind coil #1
wind coil #2
convert winding station to assembly station
assemble coil assembly # 2
install bobbin manuf tooling
lab bobbin #1
lab bobbin #2
install coil assembly tooling station
assemble coil assembly #1
install shield lab tooling
lab inner shield #1
lab outer shield # 1
lab inner shield # 2
lab outer shield #2
install vac vessel lab tooling
lab outer vac vessel #1
lab inner vac vessel #1
lab outer vac vessel # 2
lab inner vac vessel #2
install test stand and tooling
complete and test coil assy #1
complete and test coil assy #2
mag coil assys completed
Earliest Start
Duration
GEM Magnet Assembly Schedule CVJ III 8/27/91
Latest Finish
Slack

FIG. 1

FIG. 2

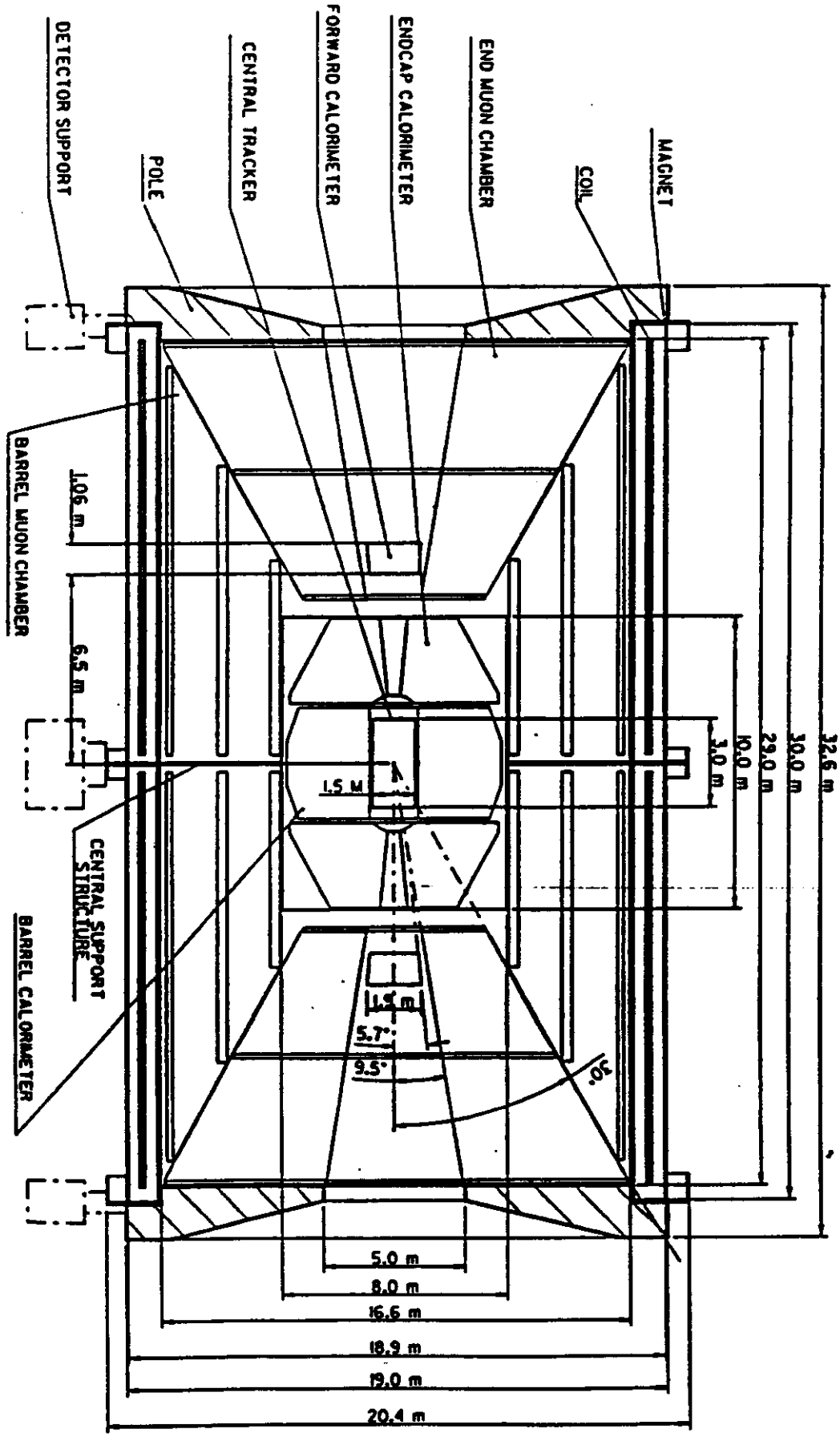
MAGNET
COIL
END MUON CHAMBER
ENDCAP CALORIMETER
FORWARD CALORIMETER
CENTRAL TRACKER
POLE
DETECTOR SUPPORT
BARREL MUON CHAMBER
1.06 m
6.5 m
CENTRAL SUPPORT STRUCTURE
BARREL CALORIMETER
1.5 M
1.5 m
5.7°
9.5°
30°
3.0 m
10.0 m
23.0 m
30.0 m
32.6 m
5.0 m
8.0 m
16.6 m
18.9 m
19.0 m
20.4 m

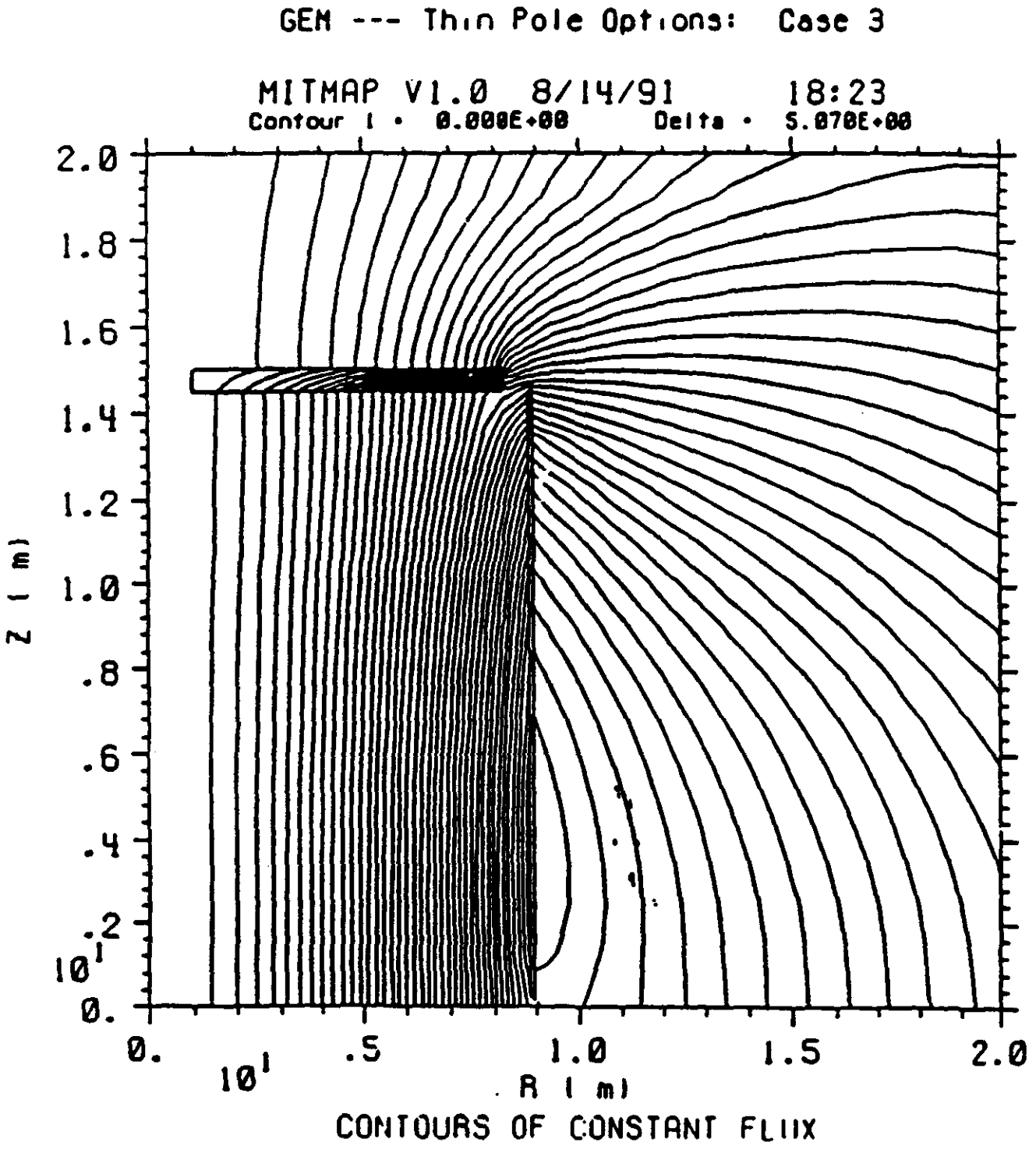
GEM --- Thin Pole Options: Case 3
MITMAP V1.0 8/14/91 18:23
Contour 1 • 0.000E+00 Delta • 5.070E+00
2.0
1.8
1.6
1.4
1.2
1.0
.8
.6
.4
.2
10¹
0.
Z (m)
0.
10¹
.5
1.0
1.5
2.0
R (m)
CONTOURS OF CONSTANT FLUX

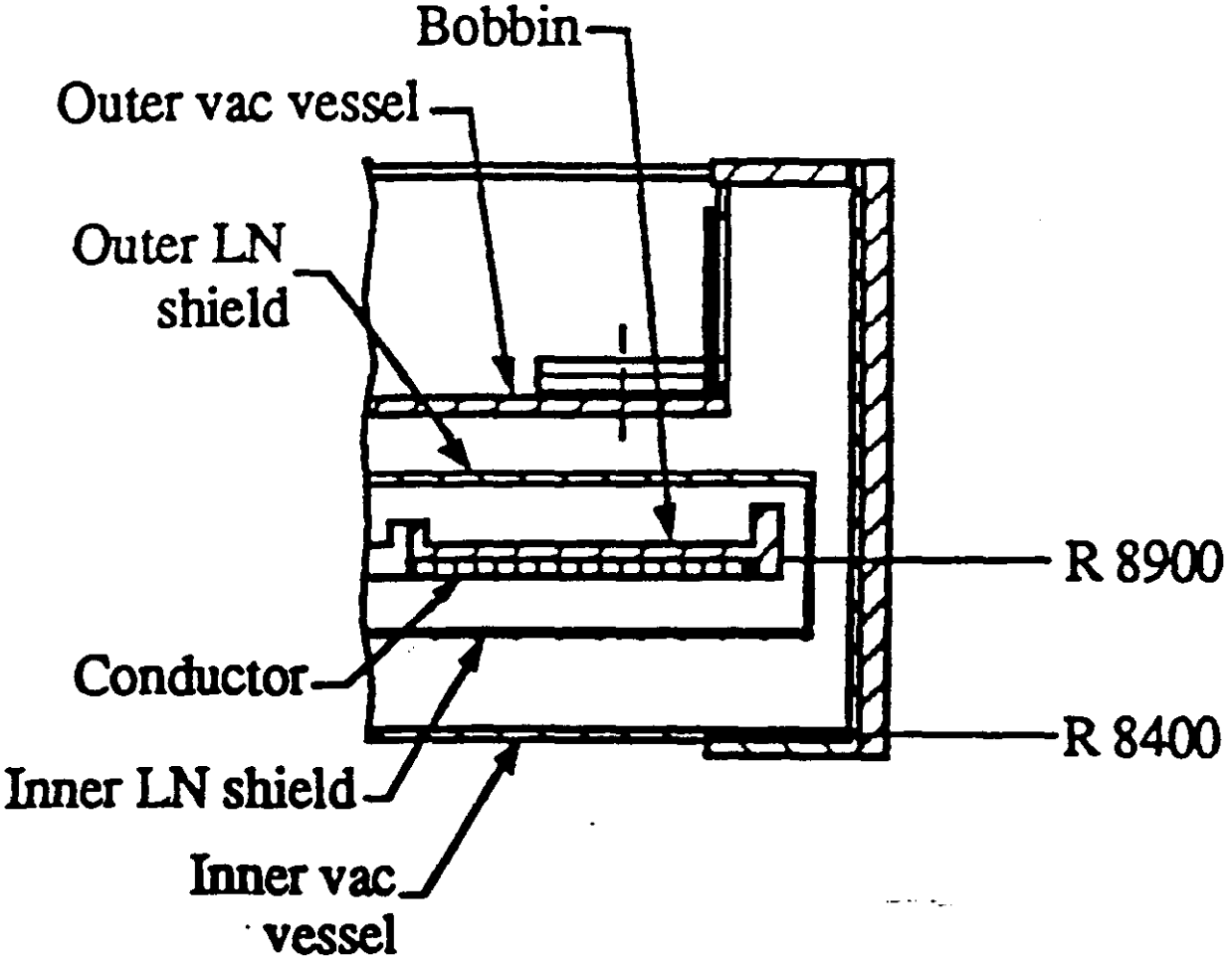
Bobbin
Outer vac vessel
Outer LN shield
R 8900
Conductor
R 8400
Inner LN shield
Inner vac vessel

FIG. 5

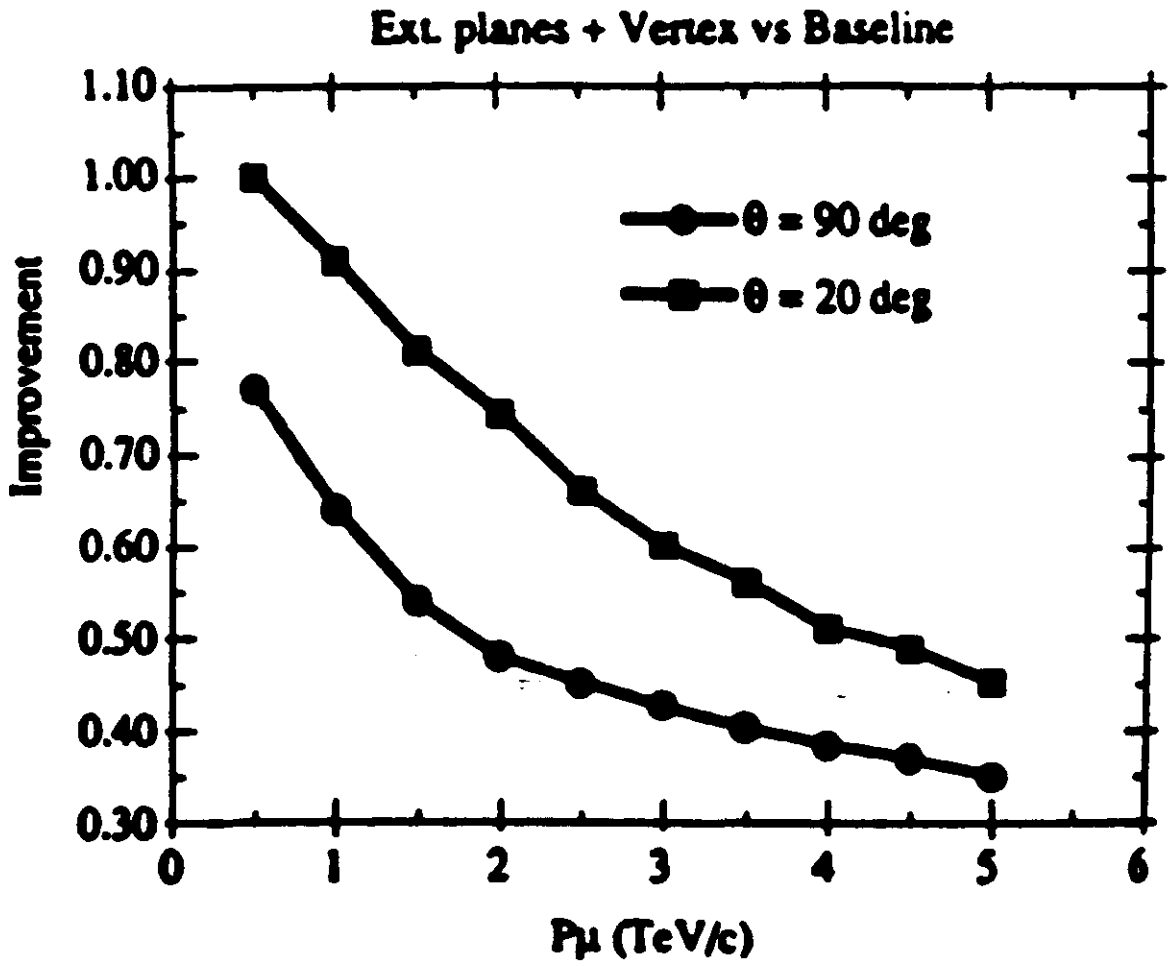
Ext. planes + Vertex vs Baseline
1.10
1.00
0.90
0.80
0.70
0.60
0.50
0.40
0.30
Improvement
θ = 90 deg
θ = 20 deg
0
1
2
3
4
5
6
Pμ (TeV/c)

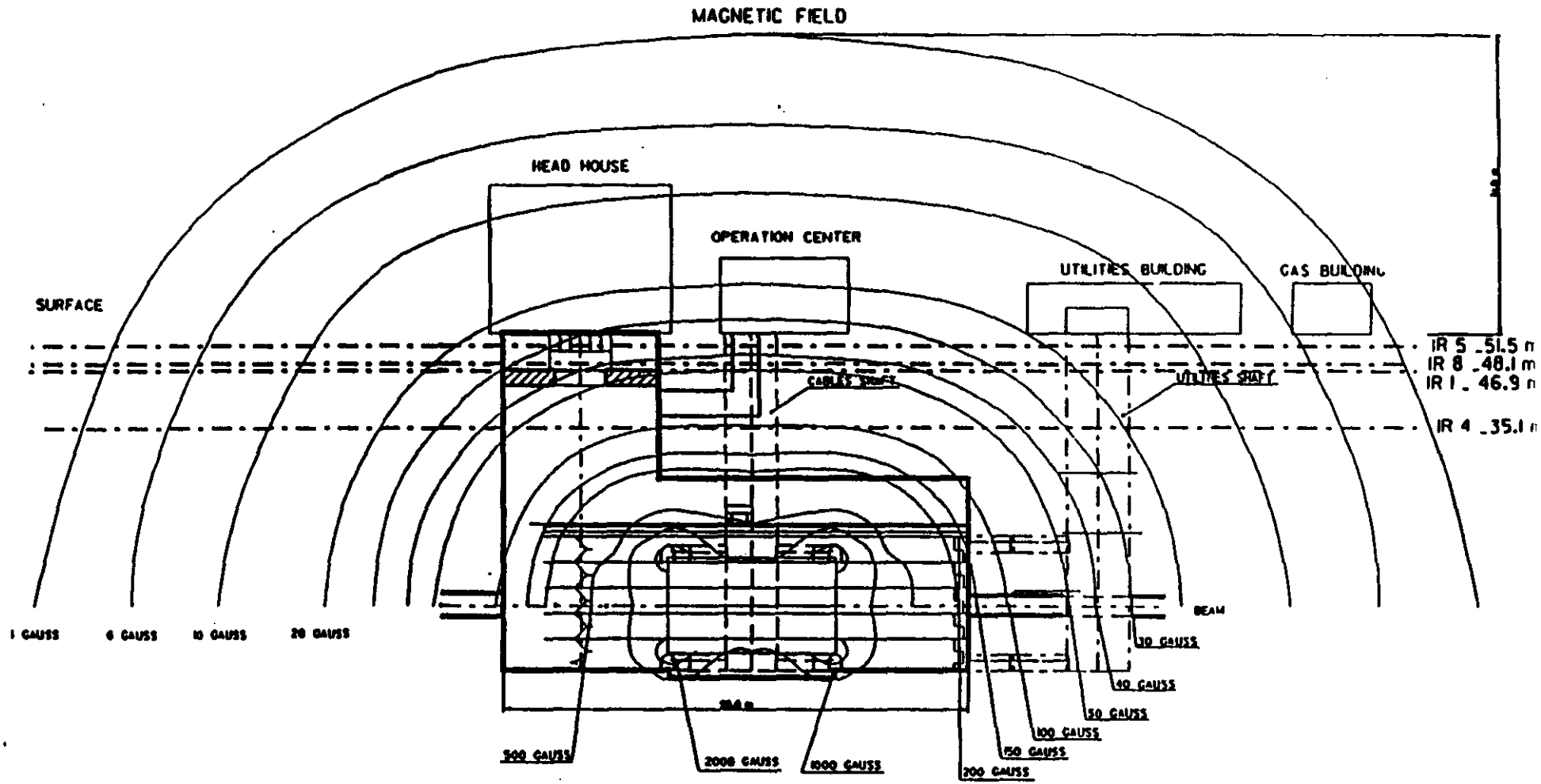
MAGNETIC FIELD
HEAD HOUSE
OPERATION CENTER
UTILITIES BUILDING
GAS BUILDING
SURFACE
IR 5 _51.5 m
IR 8 _48.1 m
IR 1 _ 46.9 m
IR 4 _35.1 m
CABLES SHAFT
UTILITIES SHAFT
BEAM
1 GAUSS
6 GAUSS
10 GAUSS
20 GAUSS
30 GAUSS
40 GAUSS
50 GAUSS
100 GAUSS
150 GAUSS
200 GAUSS
500 GAUSS
2000 GAUSS
1000 GAUSS

FIG. 6

FIG. 7

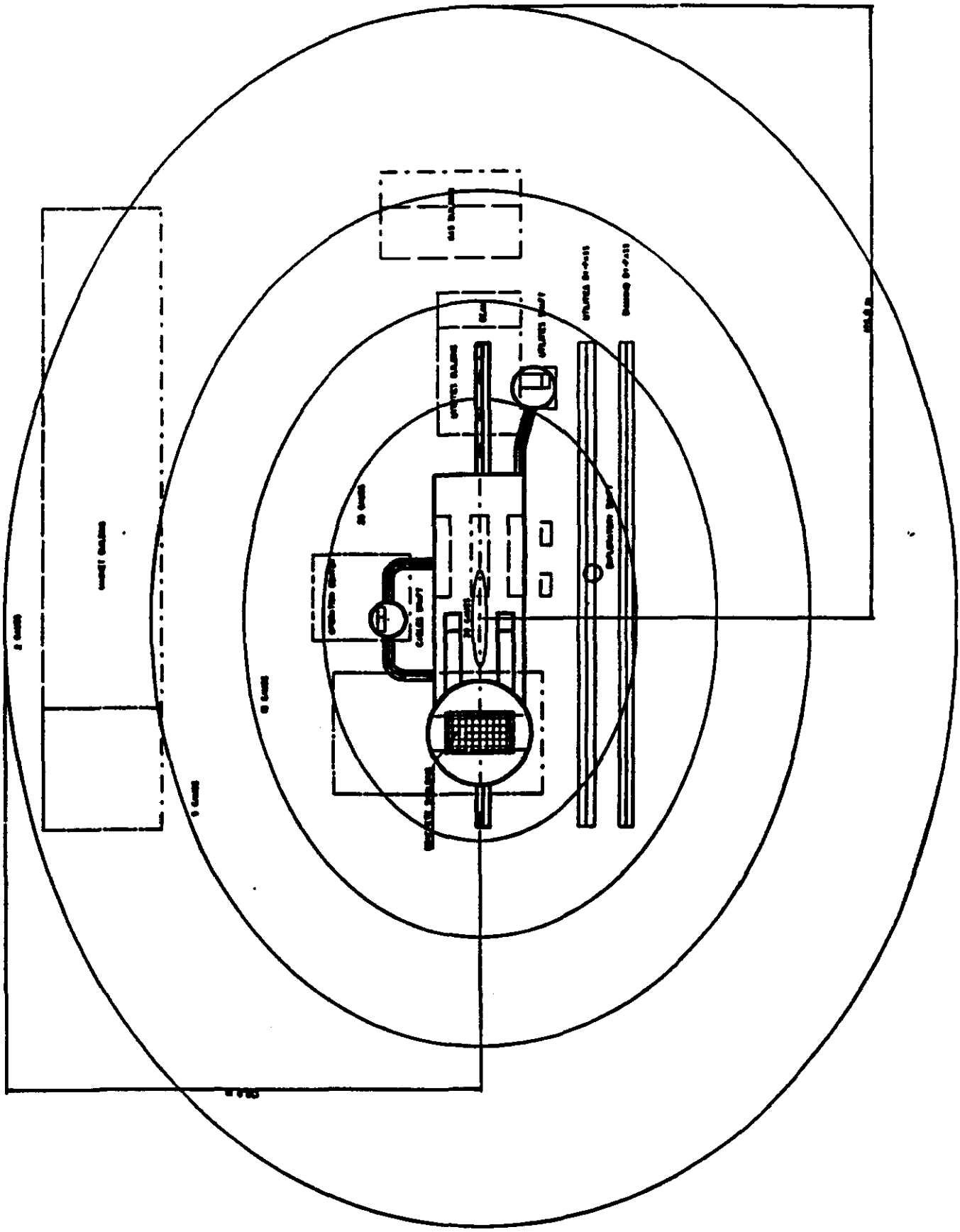

FIELD SIZE COMPARISON

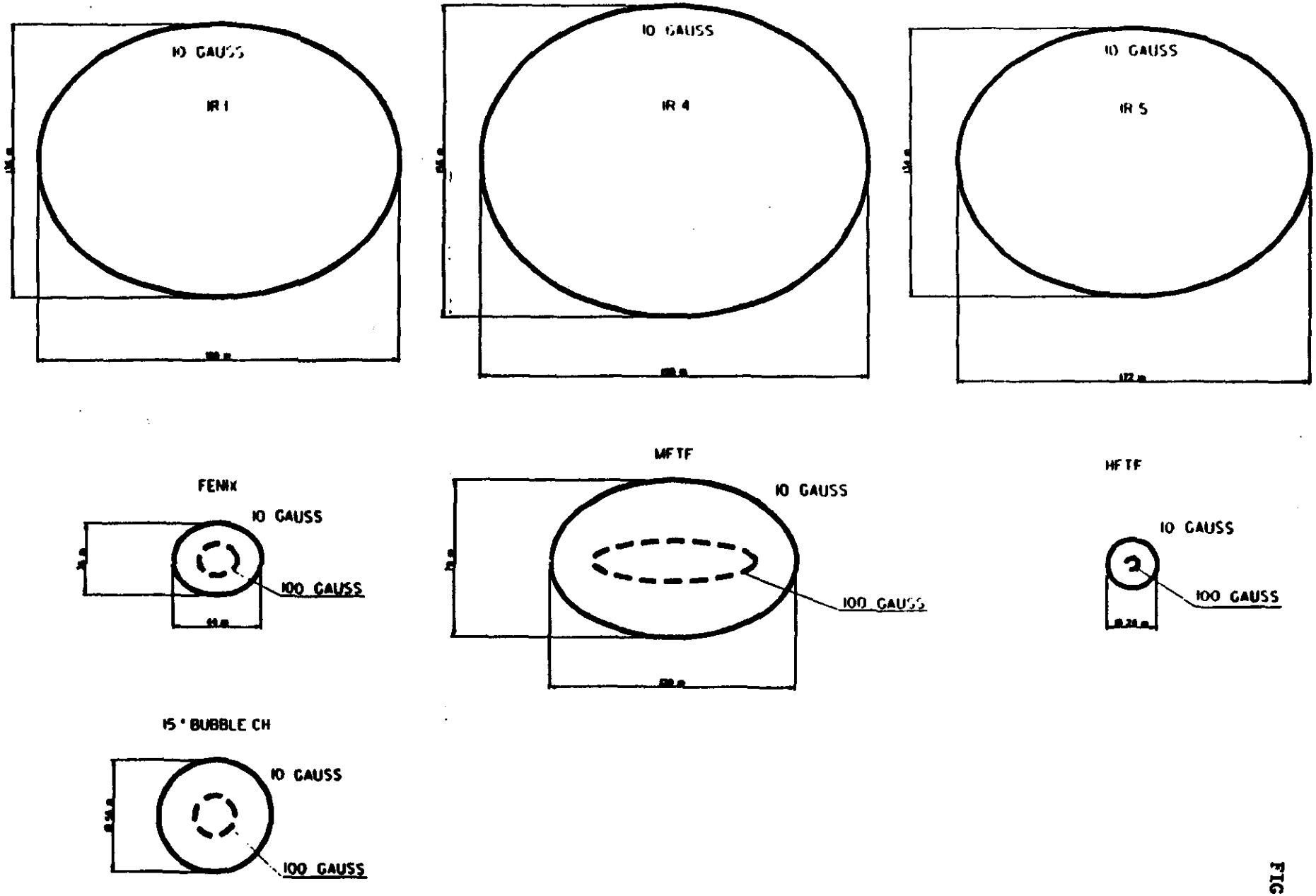

FIG.

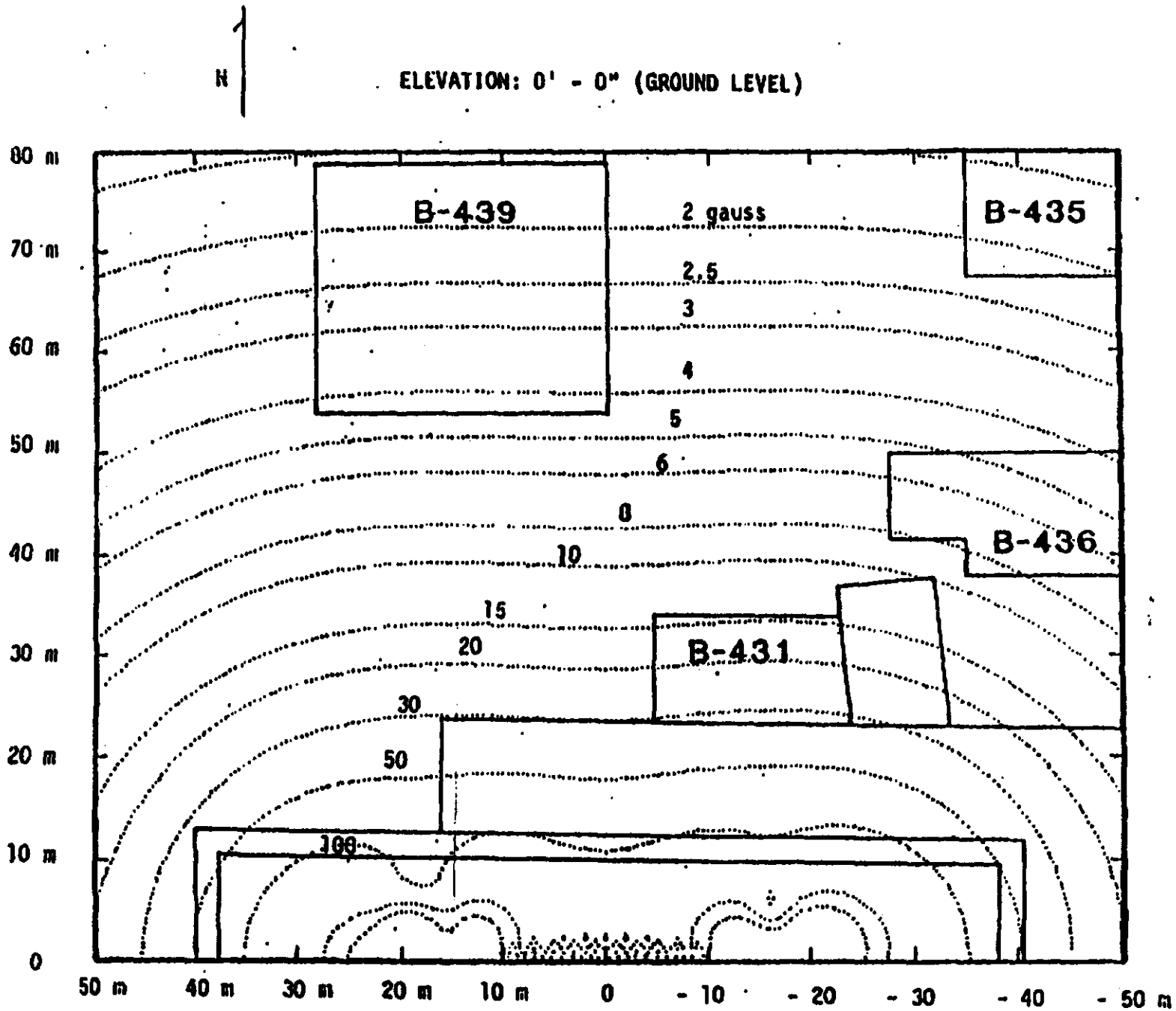
N
ELEVATION: 0' - 0" (GROUND LEVEL)
B-439
B-435
B-436
B-431
2 gauss
2.5
3
4
5
6
8
10
15
20
30
50
100
80 m
70 m
60 m
50 m
40 m
30 m
20 m
10 m
0
50 m
40 m
30 m
20 m
10 m
0
- 10
- 20
- 30
- 40
- 50 m

SSC GEM DETECTOR—BASELINE OPTION
SOLDESIGN V3.0 10/ 8/91

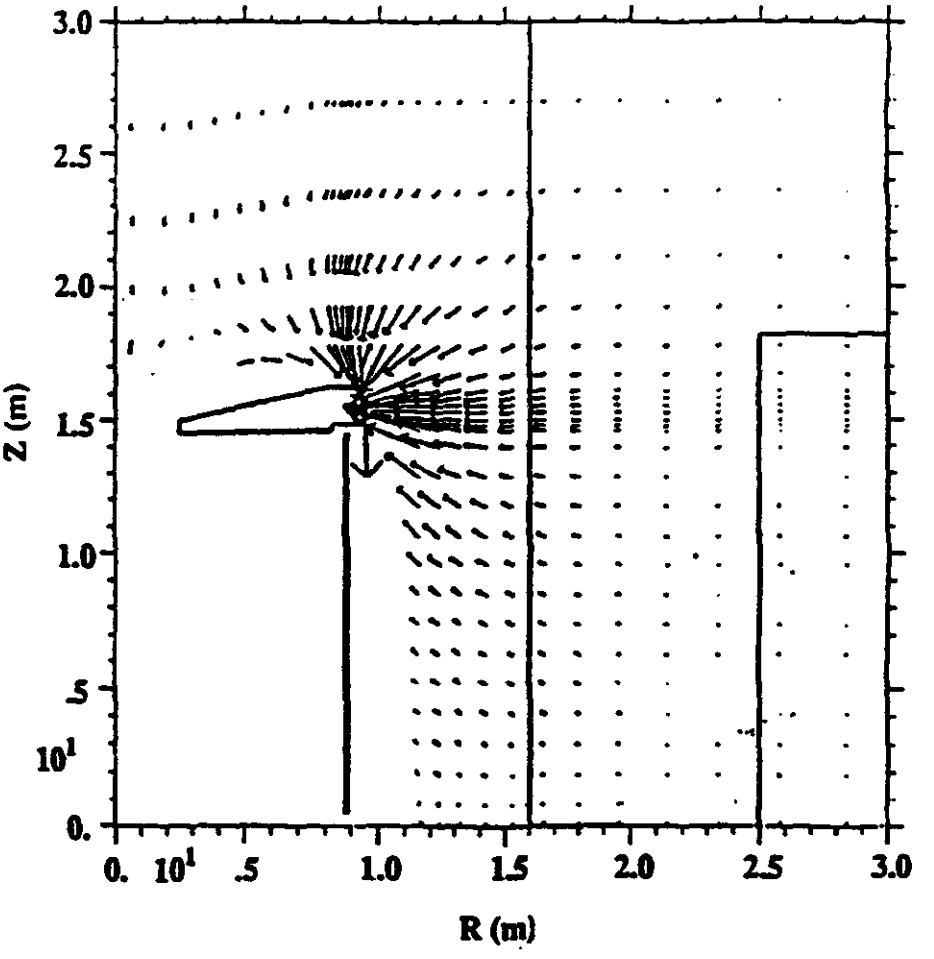

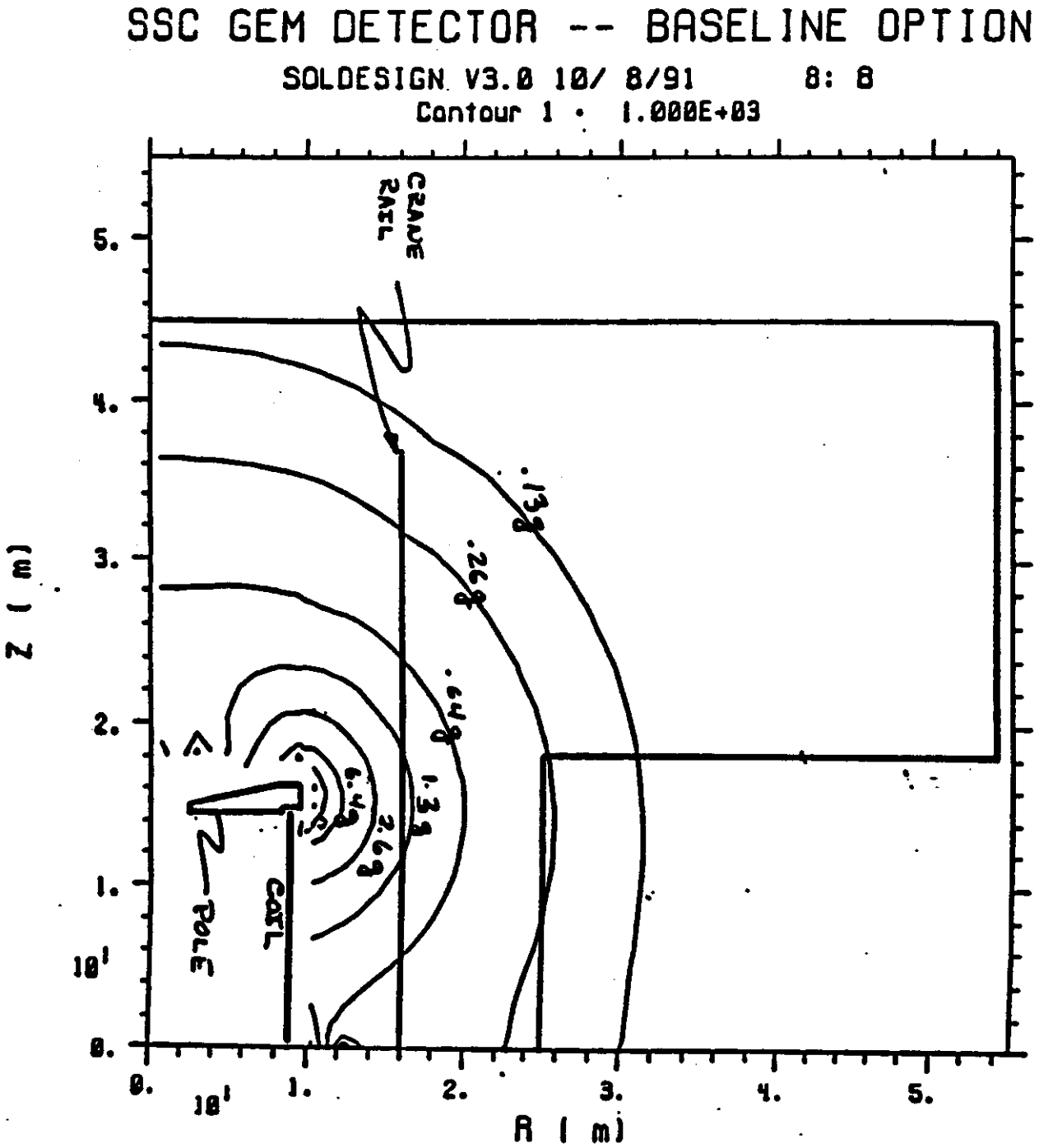
SSC GEM DETECTOR -- BASELINE OPTION
SOLDESIGN V3.0 10/ 8/91 8: 8
Contour 1 : 1.000E+03
CRANE RAIL
POLE
COIL
.13T
.26T
.64T
1.3T
2.6T
6.4T
Z (m)
R (m)
0.
1.
2.
3.
4.
5.
10¹

APPENDIX 1

FRINGE FIELD DIPOLE-DIPOLE FORCE INTERACTION

APPENDIX 1

MIT-GEM-EM-01

Fringe Field Dipole-dipole Force Interaction

05 November 1991

R. D. Pillsbury, Jr.

This document and all reports and memoranda in this series are intended as a record of MIT work in progress. They are for use in informal discussions of design and fabrication alternatives. This material is subject to change and should not, therefore, be published or referred to in the open literature. Conclusions are preliminary and distribution should be strictly limited.

Plasma Fusion Center
Massachusetts Institute of Technology
Cambridge, MA 02139

TO: R. J. Thome

FROM: R. D. Pillsbury, Jr.

DATE: October 31, 1991

SUBJECT: Fringe Field Dipole-dipole Force Interactions

INTRODUCTION AND SUMMARY

A force and possibly a torque are experienced by magnetizable material when placed in a magnetic field. Initial estimates of the magnitudes and directions of the forces arising from an interaction of such material with the fringe fields of the magnet for the GEM detector have been made and are described below.

Several magnet pole and return frame design options have been investigated. These are: (1) the thin pole with no flux return frame; (2) the thick pole with no return frame; and (3) the thick pole with a 1.8 m thick return frame.

The body force densities experienced by small volumes of magnetizable material vary from less than 1 kN/m**3 to a maximum of 20 kN/m**3 (except for a small region in the vicinity of the pole where the forces are higher). In terms of the acceleration of gravity for iron at 7800 kg/m**3 the range is from 0.1 to 2.5 g's. For installed structural components such as rock bolts and I-beams, these forces appear to be a small portion of the total load carrying requirements.

For the two designs without a return frame, the forces are very similar with differences only in the immediate vicinity of the pole. The iron return frame serves to shield the hall from the fields and, hence, the force distributions are reduced by a factor of approximately 20 over the other two cases.

ALGORITHMS

If the volume of material is small so that its influence on the local field is negligible, the body force density can be expressed as:

$$\vec{F} = (\vec{M} \cdot \vec{\nabla})\vec{B} \tag{1}$$

where $\vec{M}$ is the magnetization in the material (i.e. the dipole moment per unit volume) and

$\vec{B}$ is a magnetic flux density. If the material magnetization vector is unable to align with the local magnetic field direction, the volume of magnetizable material will also experience a torque that tends to align the magnetization direction and the ambient field directions. This torque is given by:

$$\vec{T} = \vec{M} \times \vec{B} \tag{2}$$

If the material is saturated then the magnetization can be written as:

$$\vec{M} = \vec{B}_{sat}/\mu_0 \tag{3}$$

where $\vec{B}_{sat}$ is the saturation flux density for the material and μ_0 is the permeability of free space. Typical values of the saturation flux density for iron range from 1.2 to 2.0 T.

On the basis of these equations, the body force density experienced by a small magnetized body which can rotate in order that its magnetization direction is aligned with the ambient magnetic field can be written as:

$$\vec{F} = \vec{B}_{sat}/\mu_0(\vec{B}/|\vec{B}| \cdot \vec{\nabla})\vec{B} \tag{4}$$

Estimates have been made of the magnitude and direction of the force density at various points in the experimental hall using equation (4) assuming a saturation magnitude of 1.5 T. These estimates are presented below.

FORCE ESTIMATES

A two-dimensional, axisymmetric, non-linear, finite element code, MITMAP, was used to generate the magnetic field distribution for the baseline magnet concept. Equation (4) was used to calculate a distribution of the force densities in the hall assuming a 1.5 T saturation field level.

Figure 1 shows an elevation view of one half of the experimental hall with the magnet and pole piece of the thin pole design shown. Also shown is the position of the crane rail. Contours of constant body force density in kN/m**3 are shown. A small body of magnetizable material aligned with the local field line on one of these contours will experience that body force density shown. Figure 2 shows vectors of this force density for the thin pole design. The length of the vector shank is proportional to the magnitude of the force. As can be seen, regions near the end of the pole experience the largest magnitude of the force and the direction is toward the pole. The crane rail above the pole cuts the

line labeled 10 kN/m**3 in the plane of the pole which in terms of the acceleration of gravity is approximately 1.2 g.

Figure 3 shows an end view of the magnet and hall at an axial or z-directed location that is at the center of the pole piece. Shown are the crane rails and the I-beams along the walls of the hall. In this view all forces are directed radially inward toward the axis of the magnet represented by the circle. The I-beams that support the crane rails see a maximum loading of approximately 30 kN/m**3 and the load falls off as a function of vertical position to 5 kN/m**3. Rock bolts, if required, will see the same level of force densities.

Figure 4 shows a plot of the axial component of the body force density (directed along the side crane rails) versus axial position measured from the center of the magnet. As can be seen, the force is zero at $z = 0$, but an object would be in unstable equilibrium at this point – any perturbation in position will put a force on the object that will tend to move it away from the $z = 0$ position. At an axial position of approximately 15 m, the axial force is again zero. It can be seen that a perturbation about this point is stable, since an object in a position on either side of 15 m will experience a force attracting it to the 15 m point (i.e. the plane of pole piece). Figure 5 shows a similar plot for the radial component of the body force density which also reaches a maximum in the plane of the pole.

Similar analyses were made for the cases of the thick pole and the iron return frame. Figure 6 shows the elevation view of the magnet and hall with the contours of constant body force density superposed for the thick pole case. Comparison of Figures 1 and 6 show that the body force density distribution in most of the hall is essentially the same. Differences only appear very near the pole.

Figure 7 shows the force density contours in the hall for the case of a thick pole plus 1.8 m thick iron flux return frame. As can be seen the force densities are reduced by a factor of approximately 20 from those of the thin or thick pole cases.

Additional analyses are under way to assess the distribution of loads on larger components such as the I-beams, crane rails, and crane cross-rails. These components may not have a local magnetization direction that aligns with the ambient field as is assumed in the preceeding analyses, but the loads found by integrating the values found using the method described in this memo should be conservative.

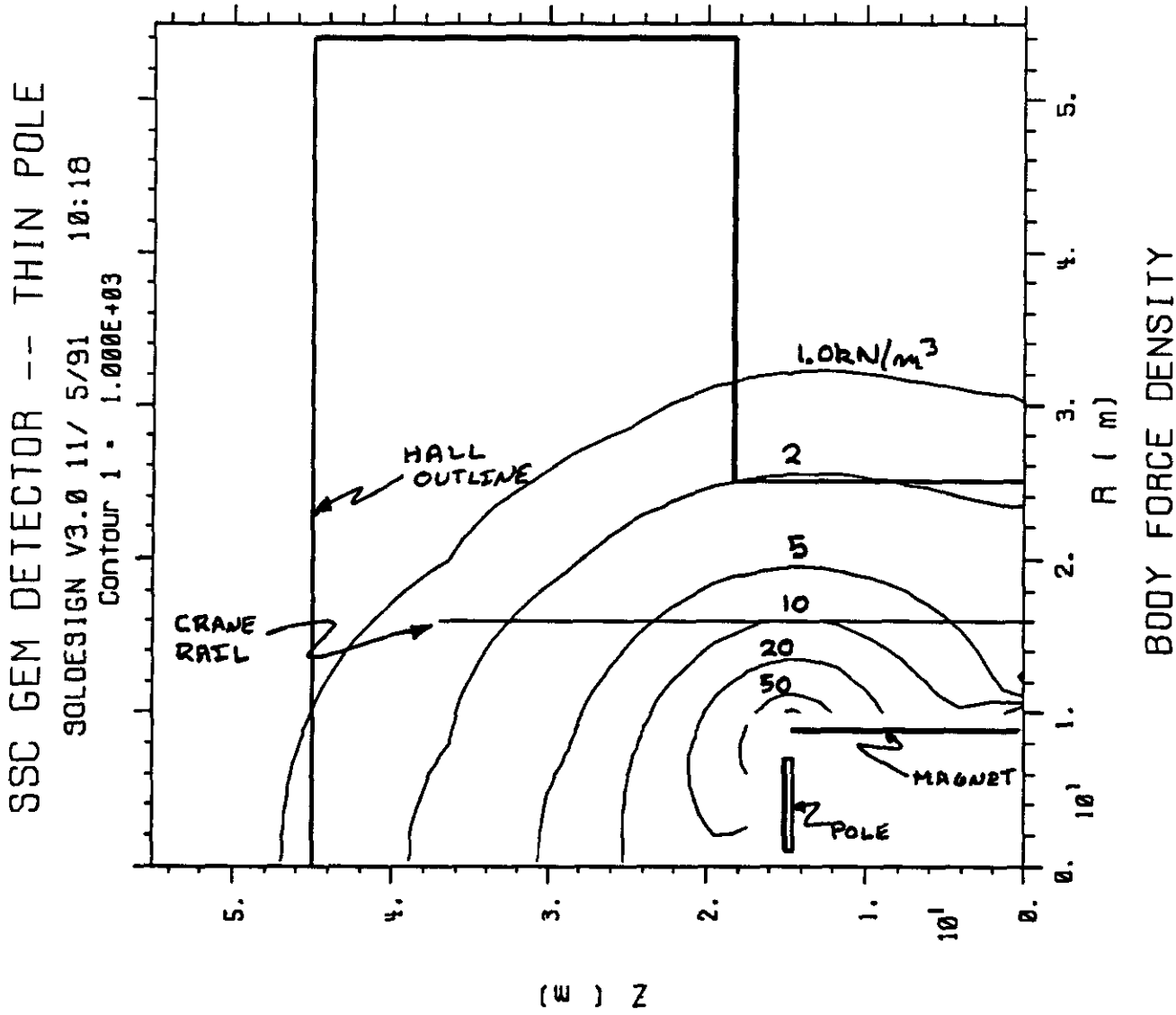

Fig. 1 – Contours of constant body force density for the thin pole baseline design for GEM. A small magnetizable body at any point along a contour will experience a body force density of the magnitude indicated. For iron at 7800 kg/m**3, 1 kN/m**3 of body force density translates to an acceleration 0.128 g's.

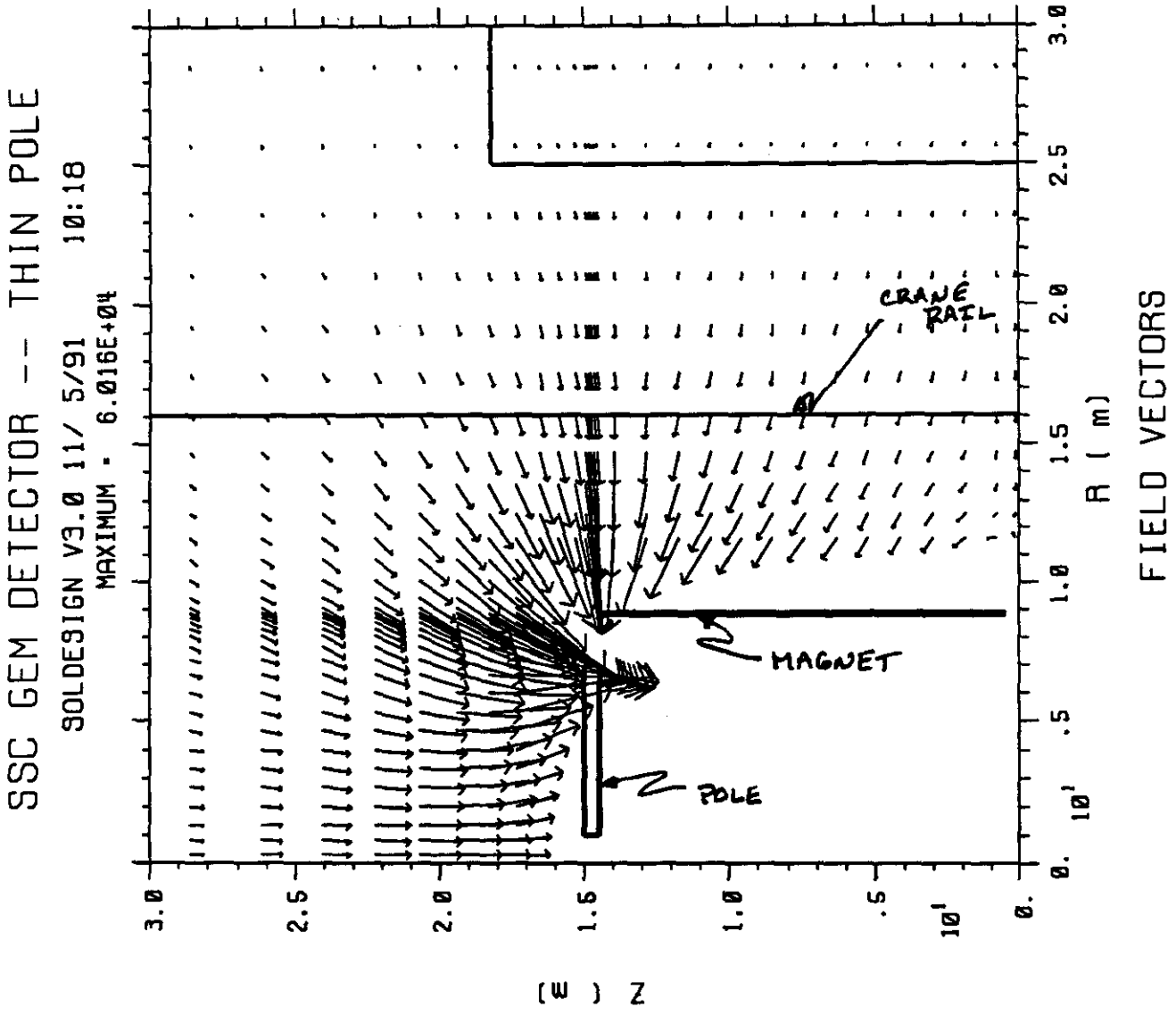

Fig. 2 – Vectors of body force density for the thin pole baseline design for GEM. The length of the vector is proportional to the force density.

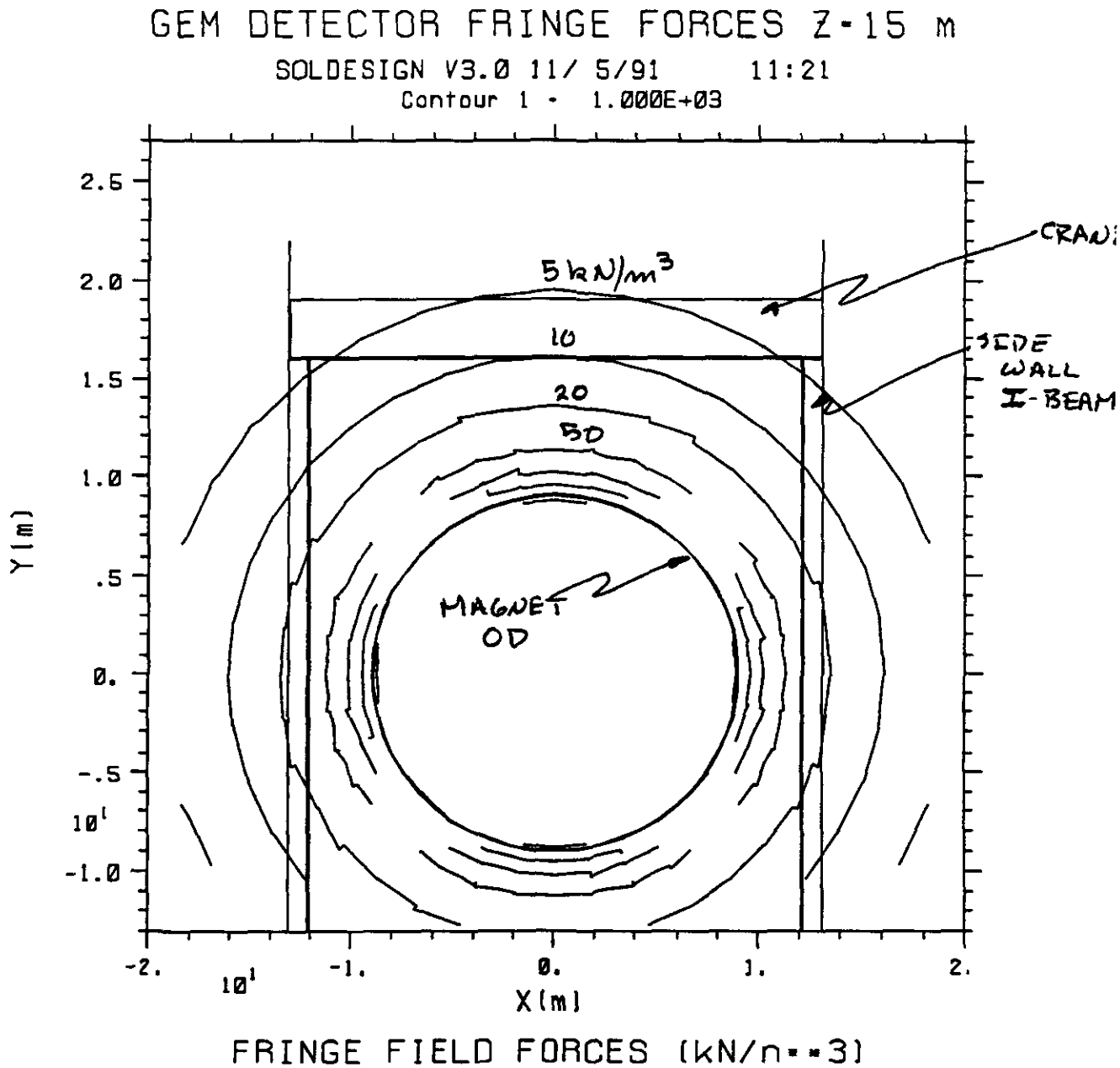

– Eigt8urs of constant body force density for the thin pole baseline design for GEM in an end view in the plane of the pole. Force direction is toward the axis of the magnet. A small magnetizable body at any point along a contour will experience a body force density of the magnitude indicated. For iron at 7800 kg/m**3, 1 kN/m**3 of body force density translates to an acceleration 0.128 g's.

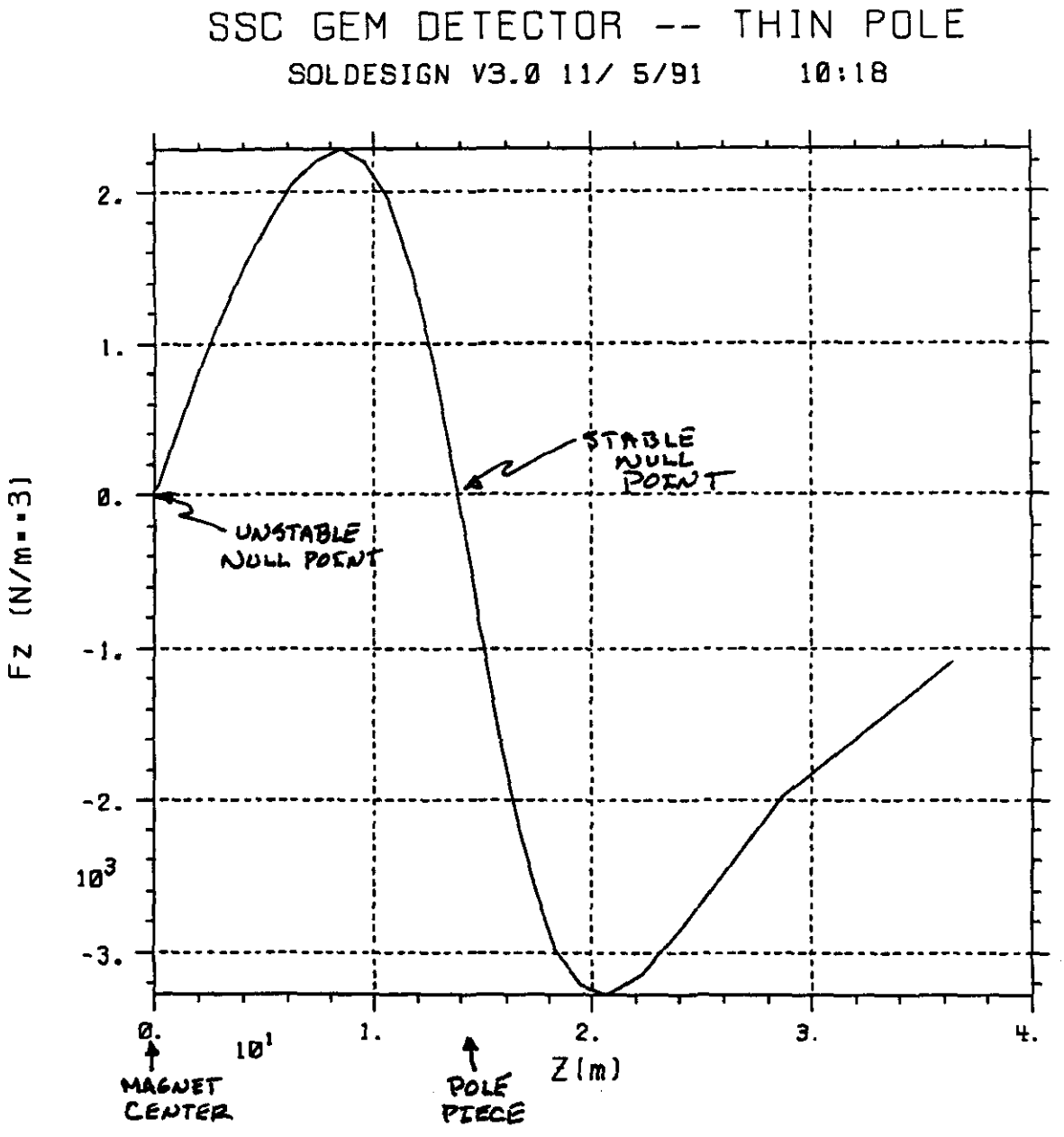

Fig. 4 – The axial component of body force density versus position along the crane rail for the thin pole baseline design for GEM.

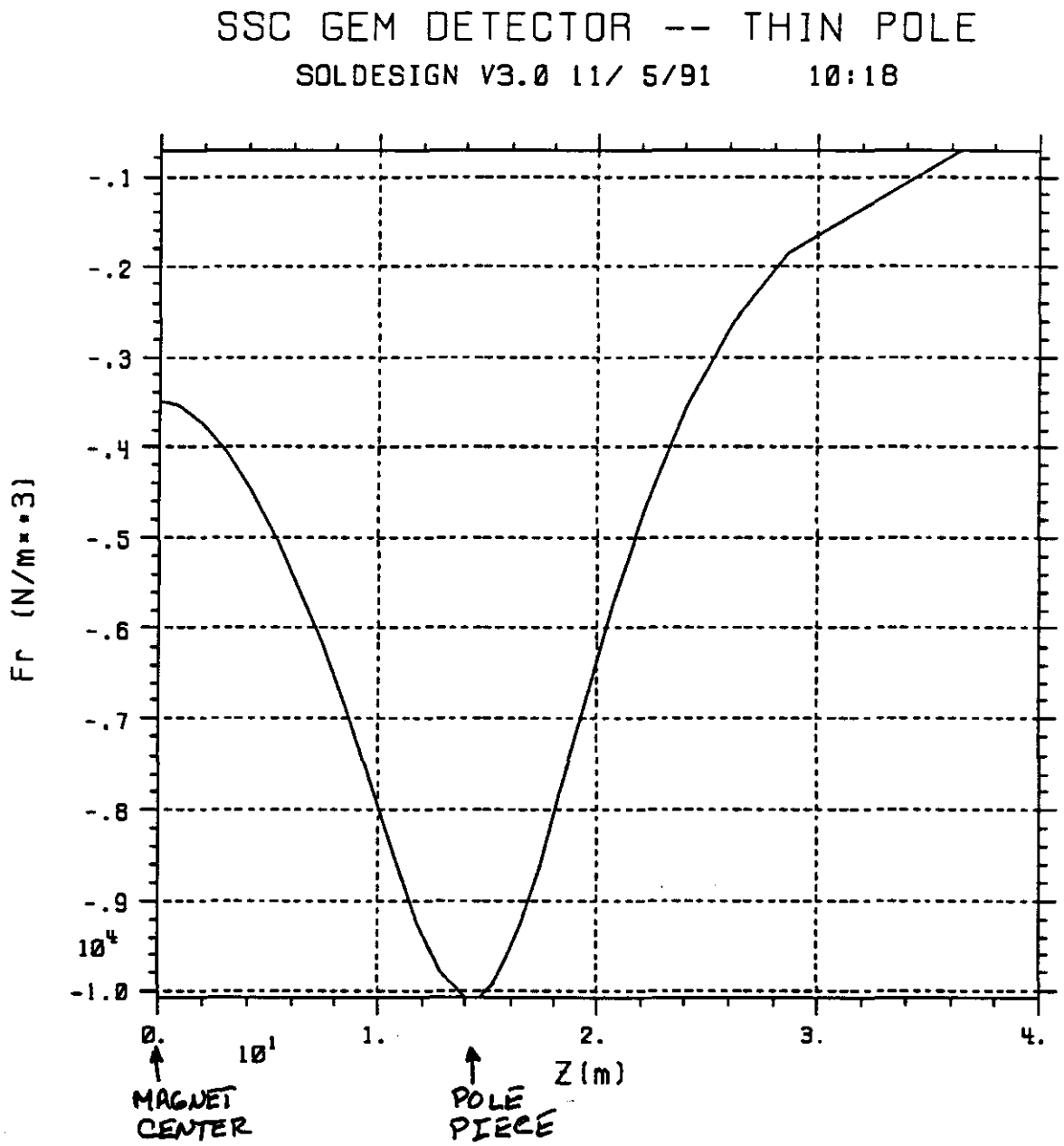

Fig. 5 – The radial component of body force density versus position along the crane rail for the thin pole baseline design for GEM.

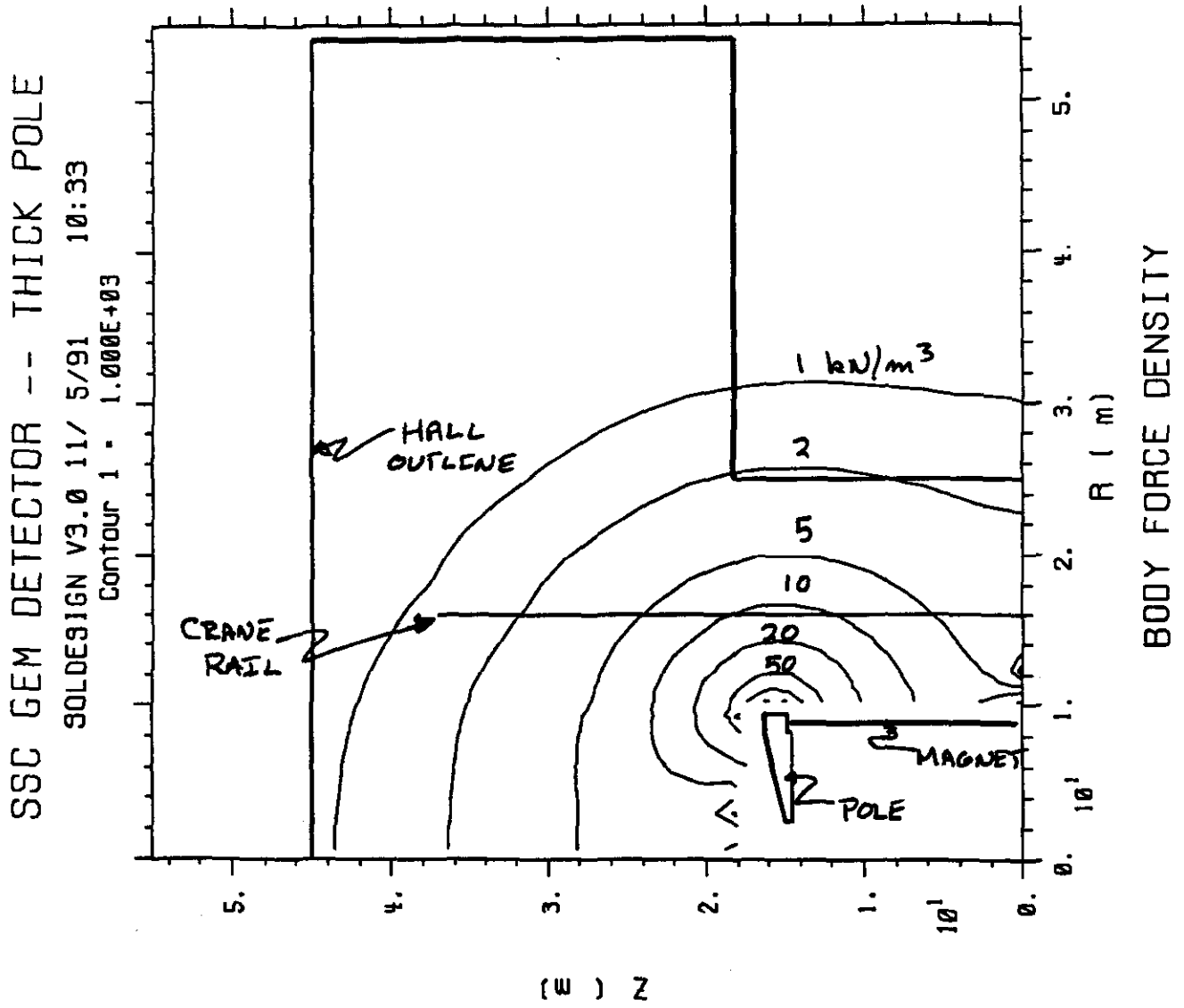

Fig. 6 – Contours of constant body force density for the thick pole design option for GEM. Note only slight differences in contours from the thin pole case.

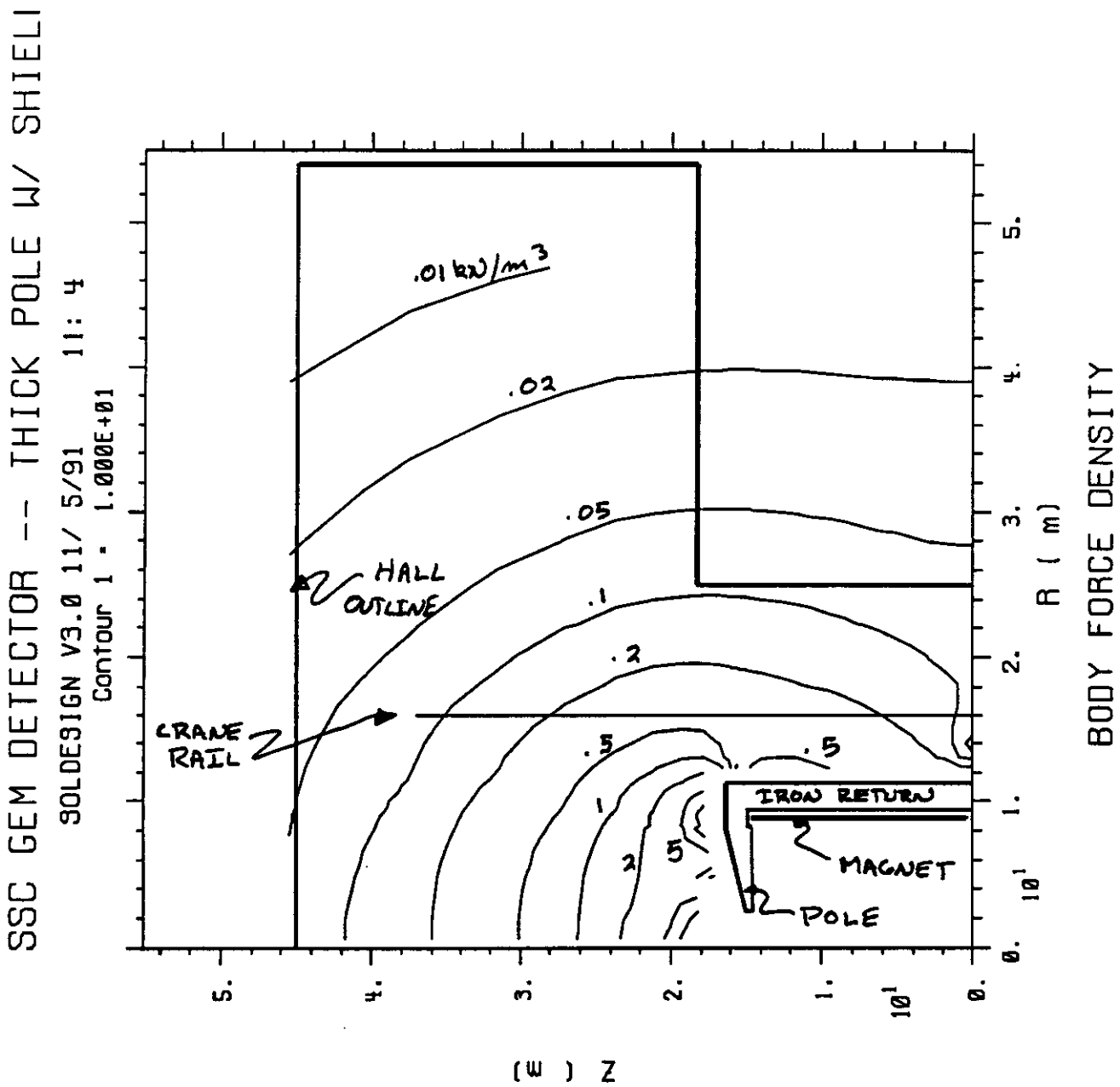

Fig. 7 – Contours of constant body force density for the iron return frame design option for GEM. Note only contours values are reduced by a factor of approximately 20 from the thin pole baseline option.

APPENDIX 2

SHIELDING OF THE MAGNETIC FIELDS FROM THE GEM MAGNET

APPENDIX 2

MIT-GEM-EM-02

Shielding of the Magnetic Fields from the GEM Magnet

7 November 1991

R. D. Pillsbury, Jr.
L. Myatt
J. Sullivan

This document and all reports and memoranda in this series are intended as a record of MIT work in progress. They are for use in informal discussions of design and fabrication alternatives. This material is subject to change and should not, therefore, be published or referred to in the open literature. Conclusions are preliminary and distribution should be strictly limited.

Plasma Fusion Center
Massachusetts Institute of Technology
Cambridge, MA 02139

TO: Distribution

FROM: R. D. Pillsbury, Jr.
L. Myatt
J. Sullivan

DATE: November 5, 1991

SUBJECT: Shielding of the Magnetic Fields from the GEM Magnet

INTRODUCTION AND SUMMARY

The present baseline design for the GEM magnet system is comprised of a single layer superconducting solenoid and a thin iron pole piece at either end. The magnetic flux density at the center of the solenoid is 0.8 T. Such a design produces significant magnetic field levels outside of the bore of the solenoid. At the surface of the earth, assumed to be 51 m above the centerline of the magnet, the field is less than 40 Gauss. The flux density at points outside the magnet system, but inside the experimental hall, varies from 2 kG to 100 G. Forces produced by the interaction of these magnetic fields with small volumes of magnetized material are discussed in a previous memorandum [1]. Field levels of this order may require the shielding of electronics and other magnet systems near the detector.

The shielding of the magnetic fields produced by the GEM magnet are described in this memorandum. Shielding requirements are investigated for two different regimes. In the first, local shielding of a region of space that sees approximately 50 G of flux density is investigated in order to assess the requirements for shielding the fields from a counting room. In the second case, the impact of shielding on the fringe fields at the surface of the earth is assessed.

For the first case, a uniform 50 G flux density is assumed and the thickness of iron necessary to reduce the flux density inside the volume of the counting room to a few Gauss is calculated. Typical results indicate that thicknesses from 50 to 10 cm will reduce the flux density to the range of 1 to 3 Gauss for the room size of 20 x 20 x 4 m assumed in the analysis.

In the second case of surface shielding, three concepts are investigated. They are:

(1) The baseline thin pole design with no iron return frame and a surface plate of iron;

(2) A thick pole design with iron return frame; and

(3) A double solenoid with a thin pole.

The fringe field distributions for each of the design options will be presented. Along with the first option, several cases of a large flat iron plate at or below the surface are analyzed. The second and third options are basically self-shielding.

The fringe field distribution from a thick pole configuration with no return frame was also calculated. As will be seen, the differences in the fringe field distributions between the thin and thick pole designs are very small except in the immediate neighborhood of the pole pieces. Therefore, minor configuration changes of the coil and pole pieces will not have a major impact on the surface or counting room shielding concepts results presented in this memo.

FRINGE FIELD DISTRIBUTIONS

Figure 1 shows an elevation view of one half of the hall, solenoid, and pole piece. A section from the magnet centerline outward is shown. Superimposed on the figure are contours of constant flux density in Gauss. As seen, in the vicinity of the pole piece, the flux density is on the order of 2 kG and falls rapidly to 0.5 kG or less over a large fraction of the hall. These axisymmetric analysis were performed using the two-dimensional, nonlinear, finite element program MITMAP [2].

Figure 2 shows a similar plot for the thick pole case. As can be seen, there are only minor differences in the fringe field in the hall except in the immediate vicinity of the pole piece. Therefore the conclusions reached concerning the shielding requirements both for the counting room and for the surface are valid for both pole piece configurations.

Figure 3 shows a similar view for a system with a thick pole and a 2.0 m thick iron return frame. As can been seen the fringe field levels are reduced everywhere. For example, the surface field has dropped from 40 G to 1 G. An alternate consisting of a 1.3 m return frame was also analyzed. The fields outside the coil bore are, of course, larger than the 2 m case, but still less than the no return frame case. For example, the flux density at the surface is 9 G.

Figure 4 shows the dual solenoid with thin pole option. This also is a self-shielded design in that the fringe fields are greatly reduced. The surface flux density is approximately 1 G.

As mentioned previously, there are several areas that may require shielding. such as the

counting room and the surface of the earth. The shielding requirements for the first case is discussed in the next section and the surface shielding is discussed in a separate section.

LOCAL SHIELDING

In order to asses the shielding requirements for regions near the magnet such as the counting room, an axisymmetric analysis was performed using ANSYS [3]. A cylindrical volume equivalent to the proposed 20 x 20 x 4 m counting room was placed in a uniform flux density of 50 G. The thicknesses of the walls and the floor and ceiling were varied independently.

Figure 5 shows a plot of the maximum flux density in the enclosed volume as a function of the floor and ceiling thickness for several different wall thicknesses. The dashed curves represent lines of constant iron volume in cubic meters. As can be seen, a 2 G field level is attainable with approximately 200 cubic meters of iron or 1560 tonnes using a 0.2 m thick wall and a 0.175 m thick floor and ceiling.

If a 1 G flux density level is required, approximately 430 cubic meters of iron or 3380 tonnes is necessary using 0.45 thick floor and ceiling and 0.30 m thick walls. Shielding to a higher level of 5 – 10 G is significantly easier and such analyses can be made when allowable flux density levels are specified.

A lower ambient flux density would allow reduced thickness with basically a linear dependence, since the iron is in unsaturated regime where the relative permeability is quite high. For example, shielding an ambient field of 5 G would require 338 tonnes of iron. However, an increase in the flux density would not scale linearly since the iron would approach saturation and the lower permeability regime is more nonlinear.

SURFACE SHIELDING

The fringe field produced by the GEM magnet at the surface of the earth has been calculated and presented in elevation views of the hall and magnet for the options discussed above.

Figure 6 shows a plan view 50 meters above the magnet with contours of constant flux density produced by the thin pole baseline. This distance corresponds approximately to the surface of the earth. The magnet is 50 meters below the surface and centered with its axis parallel to the z-axis in the figure. As can be seen, the maximum fringe field is approximately 40 G (Note: the 10^1 label).

Figure 7 shows a similar plot for the thick pole case. A comparison of figures 6 and 7

reinforces the statements made about similarity in fringe fields from the thin and thick pole cases.

Figure 8 shows the surface fringe field plot for the case of a thick pole and a 2 m thick iron return frame. As can be seen the field level is 1 G. If a 10 G field level is allowed, a thick pole and 1.3 m thick return frame is sufficient as is shown in Figure 9. Finally, Figure 10 shows the surface plot for the thin pole and a double solenoid. As can be seen, the maximum flux density is 2 G and considerably reduced in axial extent.

These figures show that surface fringe field levels of 1 to 10 G are attainable with the self-shielding options. However, there are significant cost and schedule impacts for such systems.

One alternative to full self-shielding is to install an iron plate or a sequence of plates between the coil and surface in order to shield the fringe fields. Figure 11 shows an example of such a plate. In this example, a quarter of the solenoid (with the pole piece omitted) and plate are shown. The planes of symmetry are called out. Also shown is a lip on the far end of the plate.

A range of plate locations, sizes, thickness and lips were analyzed using ANSYS. The optional lip was added to redirect the fringing of the field lines as they enter (or leave) the plate at the ends and, therefore, reduce the fields at the surface.

Table 1 lists some of the cases run, the plate geometry, the plate depth below the surface, the size of the lip, the flux density on the surface in the geometric center of the plate and the value at the edge of the plate (the fringing effect), and the iron required.

Several conclusions can be drawn from this table. They are:

(1) A plate closer to the surface will produce a higher amount of fringing over the edges of the plate at the surface. For example, runs 13, 16, and 17 show essentially the same flux density magnitude at the surface over the center of the plate but the lower plates produce between 20% and 40% of the fringing at the surface.

(2) Plates close to the surface need a lip to reduce the fringing field to a value equal to or below the level of the field at the center of the plate. For example, runs 18 and 19 show that a 5 m lip, 0.5 m thick reduces the maximum field on the surface from 11 G to 5.6 G – the flux density in the plate is well below saturation. Plates further from the surface may not require a lip at all.

(3) A 160 x 140 x 0.5 m plate with a 5 m lip that is 1.5 m below the surface shields the surface to 1.4 G except in the neighborhood of the edge where it rises to 5.6 G.

Figure 12 shows the flux density magnitude at the surface versus position along the surface at the plane of symmetry. The extent of the plate (which is 1.5 m below the surface) is indicated. As can be seen, the flux density is 1.4 G at the center and falls to 0.5 G near the edge, but the fringing of the field is evident as the magnitude rises to 5.6 Gauss at the edge. It is felt that the fringing may be further reduced to the 1.4 G level by varying the depth and thickness of the lip. This case may be compared to the 2 m thick iron return frame as shown in Table 2.

(4) A 120 x 100 x 0.15 m plate with a 5 m lip that is 1.5 m below the surface shields the surface to 8 G or less. This case can be compared with the 1.3m thick iron return frame case – see Table 2.

(5) Finally, it appears surface shielding is possible if the maximum flux density is in the 1 to 10 G range. Optimization of the plate thickness with position and of the lip may allow a reduction in the weights shown.

Table 1: Surface Shielding With Iron Plates

Plate Size (m)	Depth Below Surface	Plate Lip to Control Fringing	Peak Surface Fields		tonnes of Iron
			Over Coil	Plate Edge	
160Lx140W 0.25 thk (Run #16)	1.5 m	No Lip	2.7 G	8.2 G	43,700
160Lx140W 0.50 thk (Run #18)	1.5 m	No Lip	1.4 G	11 G	87,400
160Lx140W 0.50 thk (Run #19)	1.5 m	5 m Lip	1.4 G	5.6 G	90,100
160Lx140W 0.25 thk (Run #21)	1.5 m	5 m Lip	2.7 G	4.5 G	46,400
160Lx140W 0.15 thk (Run #23)	1.5 m	5 m Lip	5.8 G	4.1 G	28,900
120Lx100W 0.15 thk (Run #24)	1.5 m	5 m Lip	8.1 G	7.7 G	16,800
160Lx140W 0.25 thk (Run #13)	9.5 m	No Lip	3.3 G	3.6 G	43,700
160Lx140W 0.25 thk (Run #14)	9.5 m	5 m Lip	3.4 G	2.7 G	46,400
160Lx140W 0.25 thk (Run #15)	9.5 m	15 m Lip	3.5 G	2.0 G	51,900
160Lx140W 0.25 thk (Run #17)	15.5 m	No Lip	4.2 G	2.5 G	46,400

Table 2: Comparison of Return Frame and Plate Shielding Options

Shielding Hardware Description	Peak Field at Ground Elevation	tonnes of Iron
160Lx140Wx0.50 thk Plate 5 m Lip, 1.5 m Below Ground (Run #19)	1.4 G	90,100
2 m Thick Iron Return Frame	1.0 G	30,100
120Lx100Wx0.15 thk Plate 5 m Lip, 1.5 m Below Ground (Run #24)	8.1 G	16,800
1.3 m Thick Iron Return Frame	8.8 G	19,100

REFERENCES

[1] R. D. Pillsbury, Jr., "Fringe Field Dipole-dipole Force Interactions," Internal memorandum MIT-GEMEM-01, October, 1991

[2] R. D. Pillsbury, Jr., "MITMAP - MAP User's Manual,",PFC/RR-91-4, February, 1991

[3] ANSYS Revision 4.4A, Swanson Analysis Systems, Inc., Houston, PA.

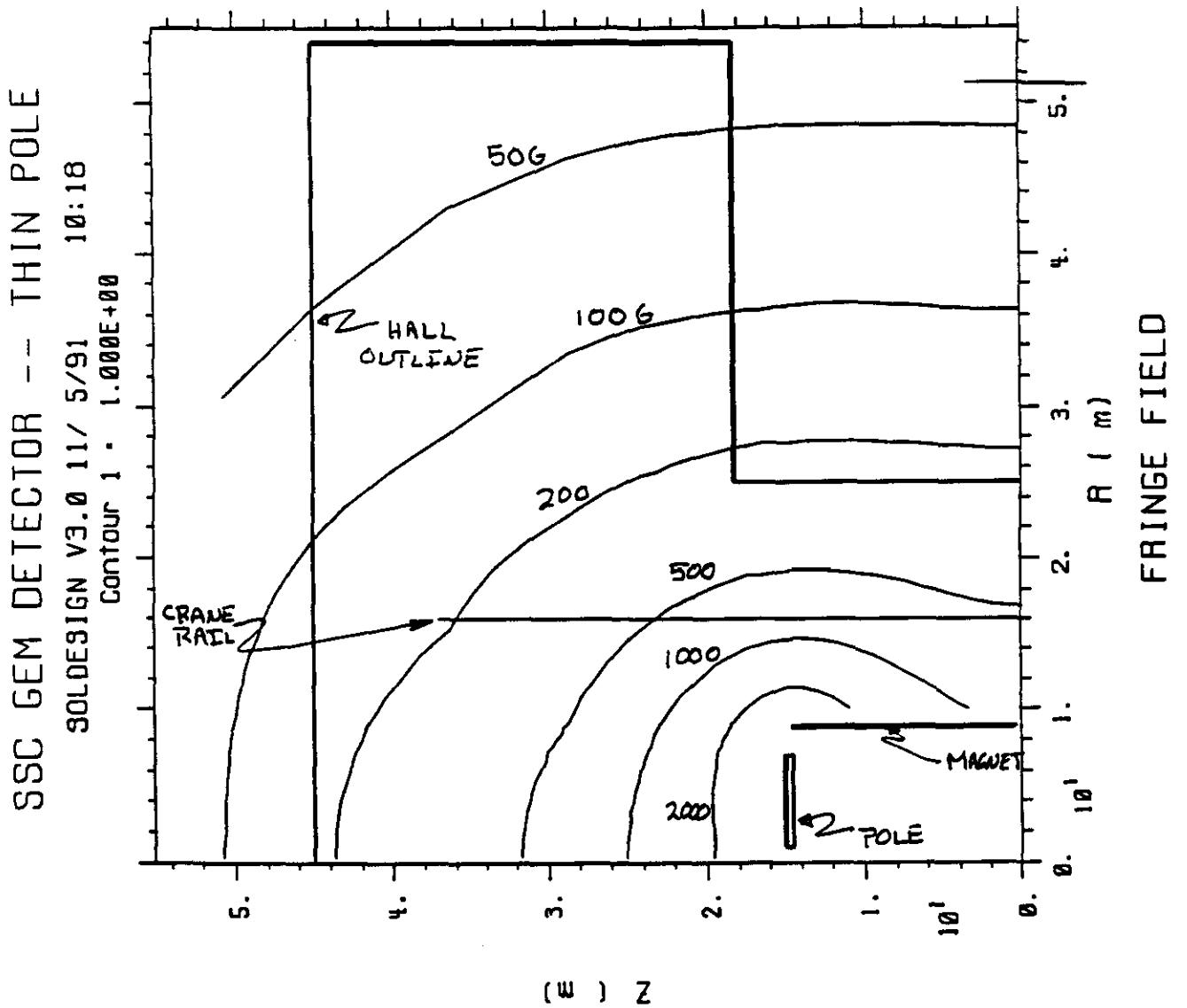

Fig. 1 – Contours of constant flux density for the thin pole baseline design for GEM superimposed on an elevation view of the experimental hall.

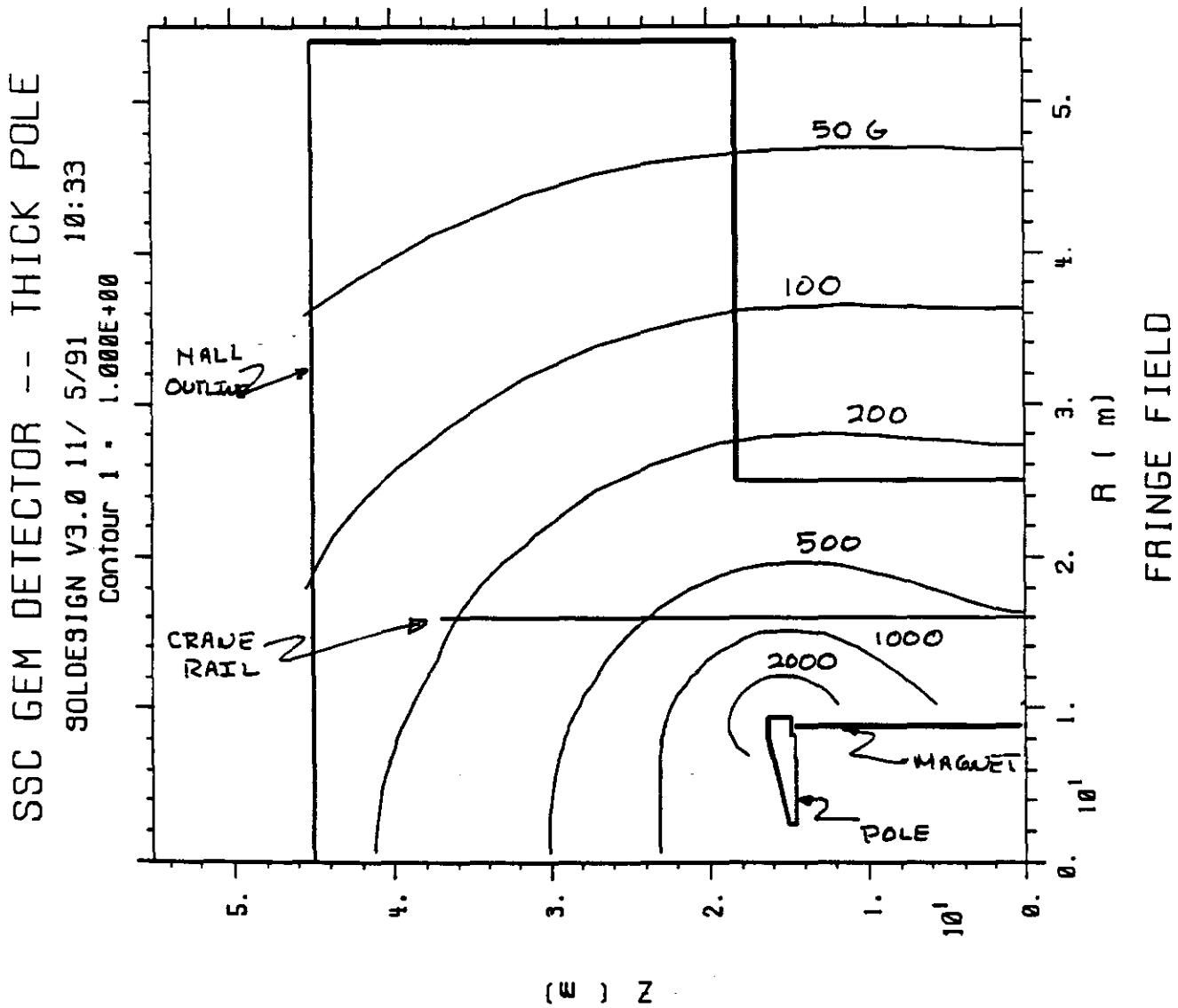

Fig. 2 – Contours of constant flux density for the thick pole design for GEM superimposed on an elevation view of the experimental hall.

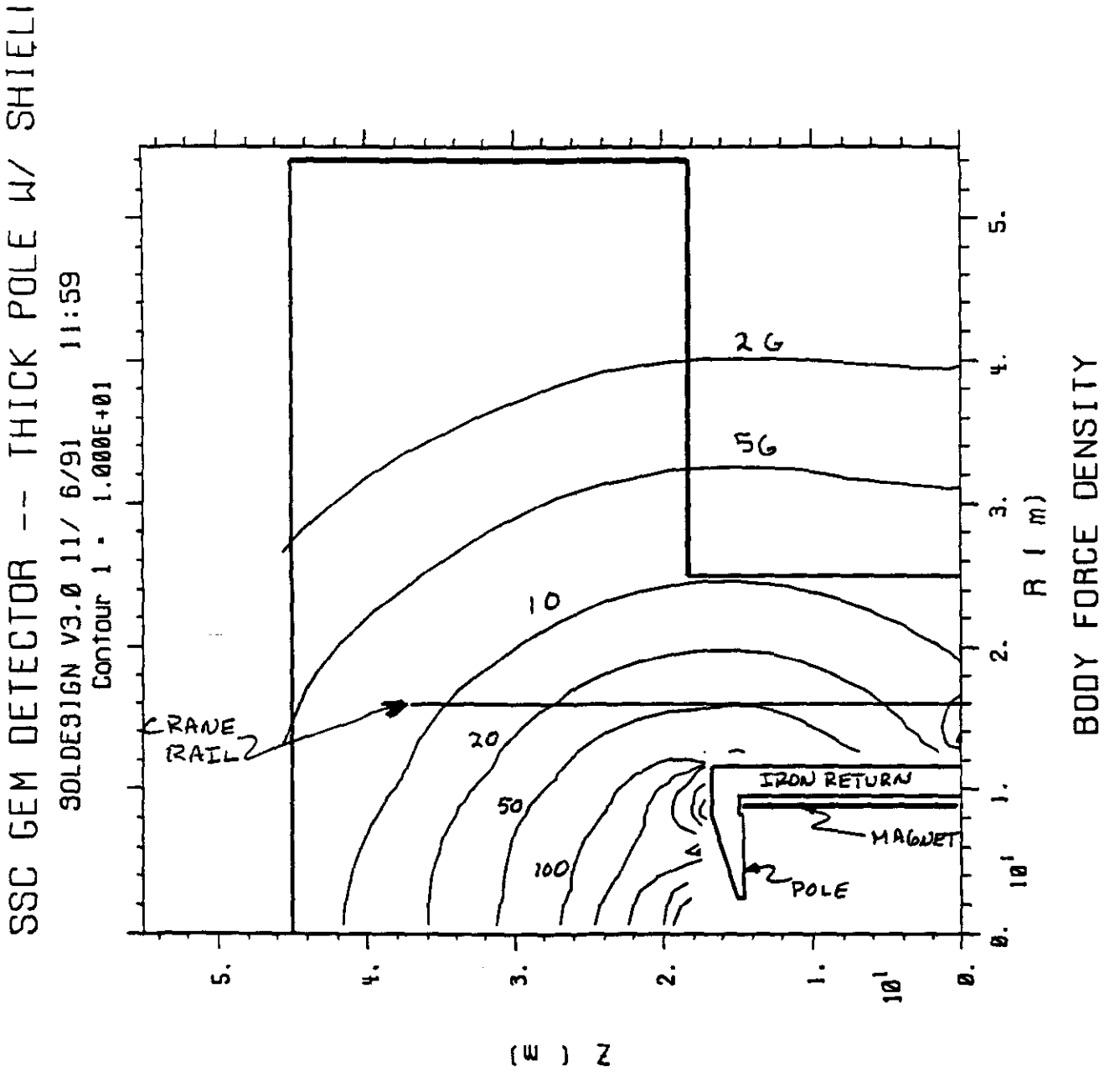

Fig. 3 – Contours of constant flux density for the thick pole and 2 m thick iron return frame design for GEM superimposed on an elevation view of the experimental hall.

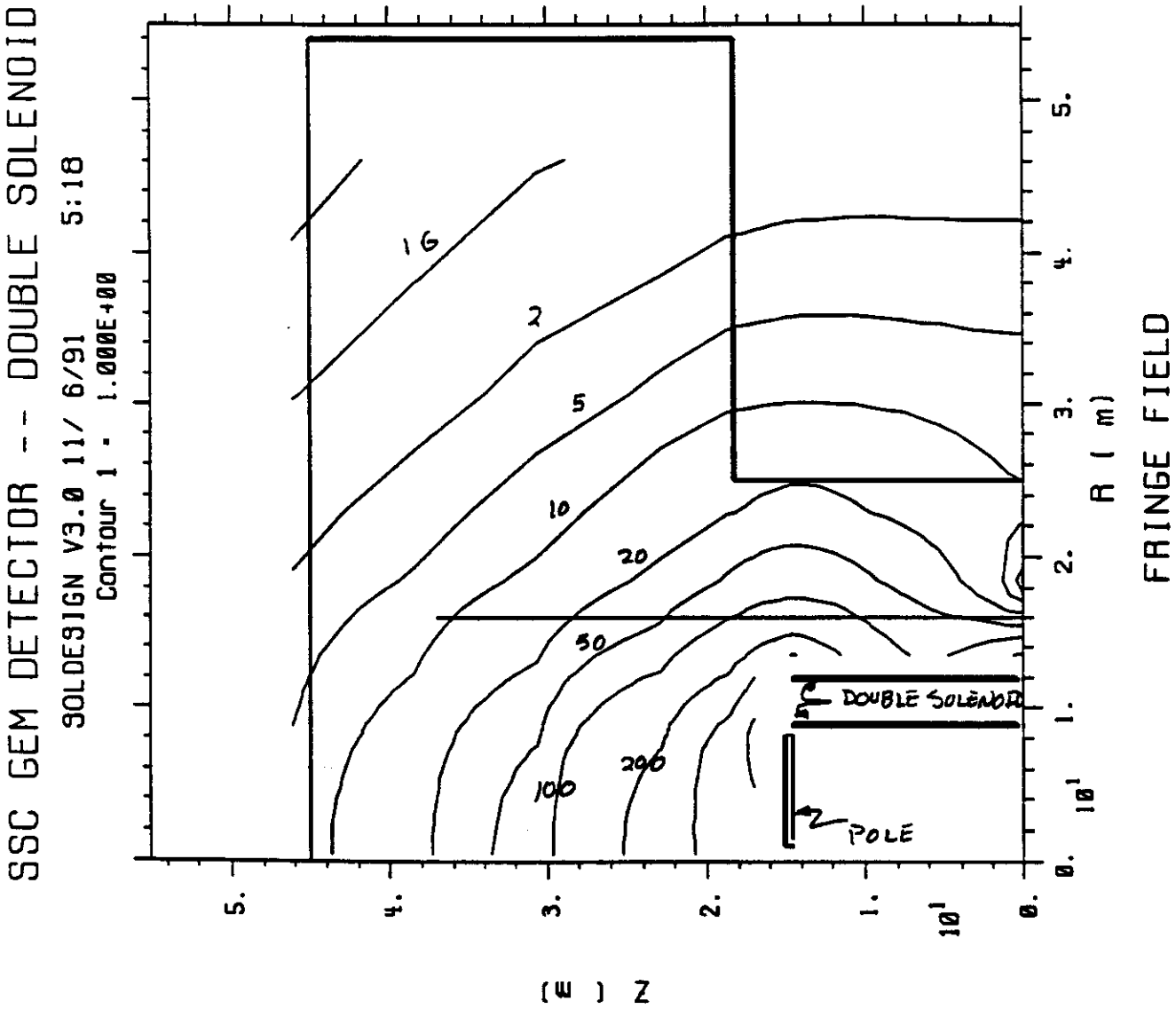

Fig. 4 – Contours of constant flux density for the thin pole and double solenoid design for GEM superimposed on an elevation view of the experimental hall.

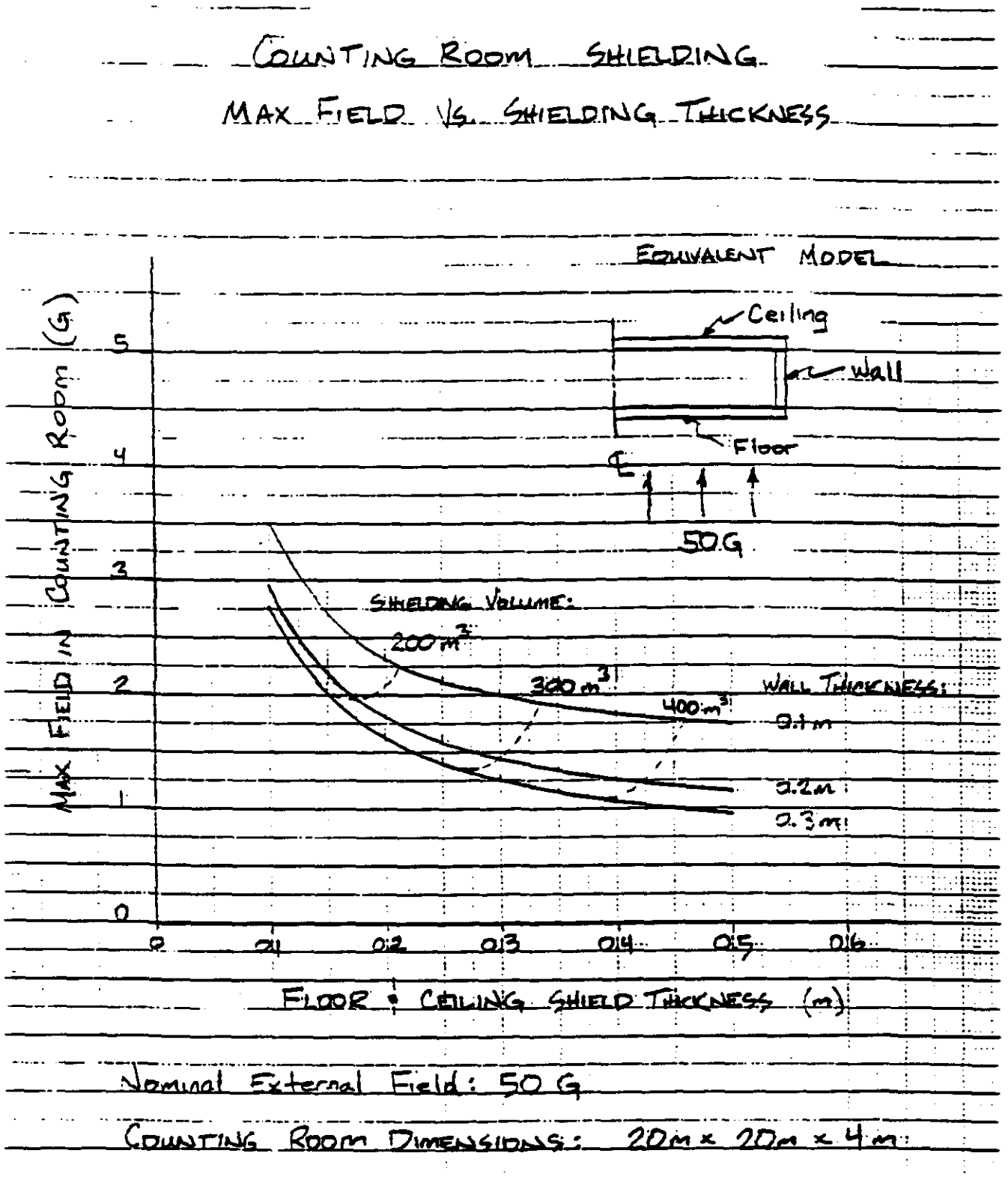

Fig. 5 – Flux density level inside a 20 x 20 x 4 m volume in a uniform 50 G field as a function of floor, ceiling and wall thicknesses.

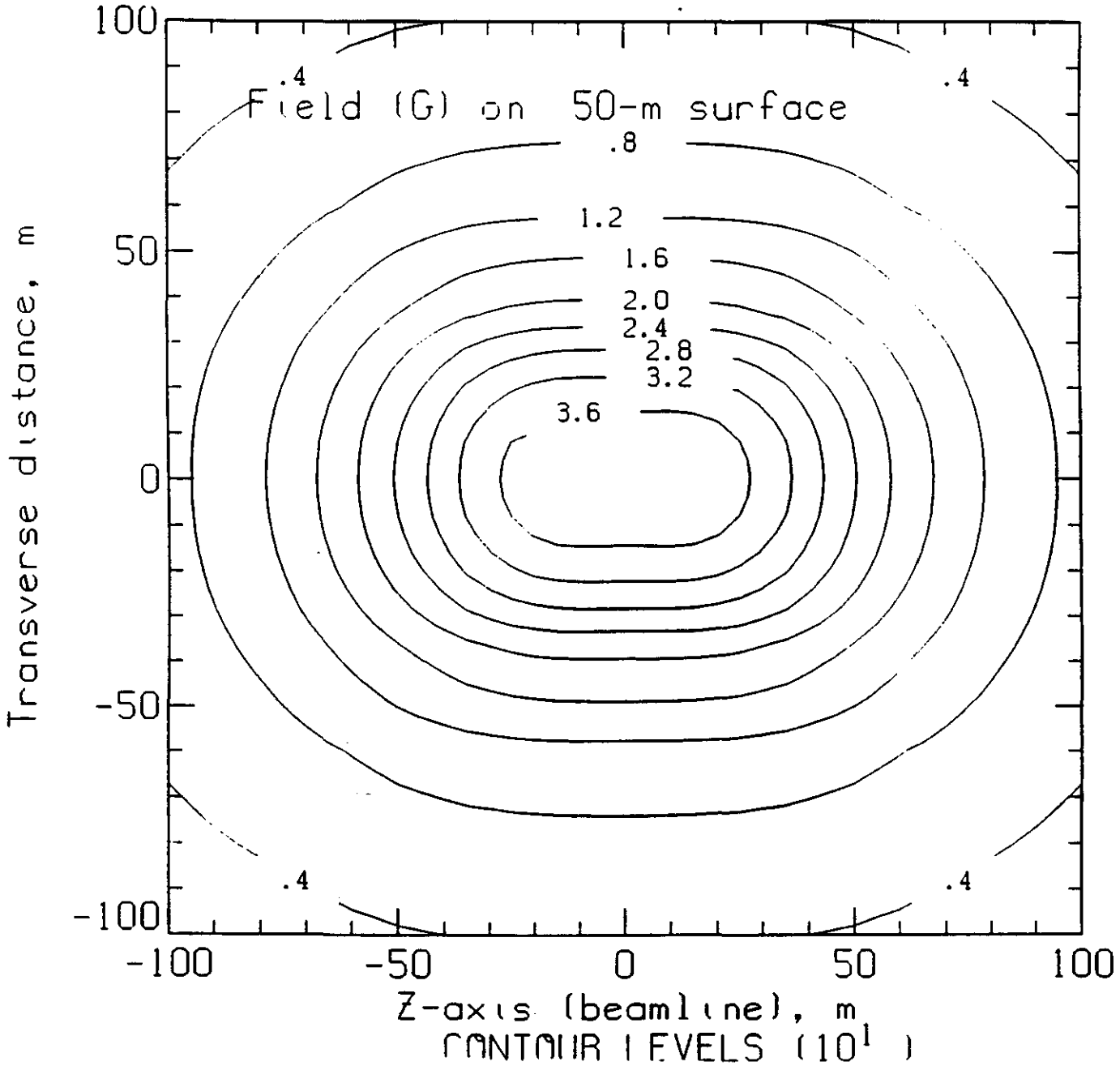

Fig. 6 – Contours of constant flux density at the surface of the earth for the thin pole baseline design for GEM.

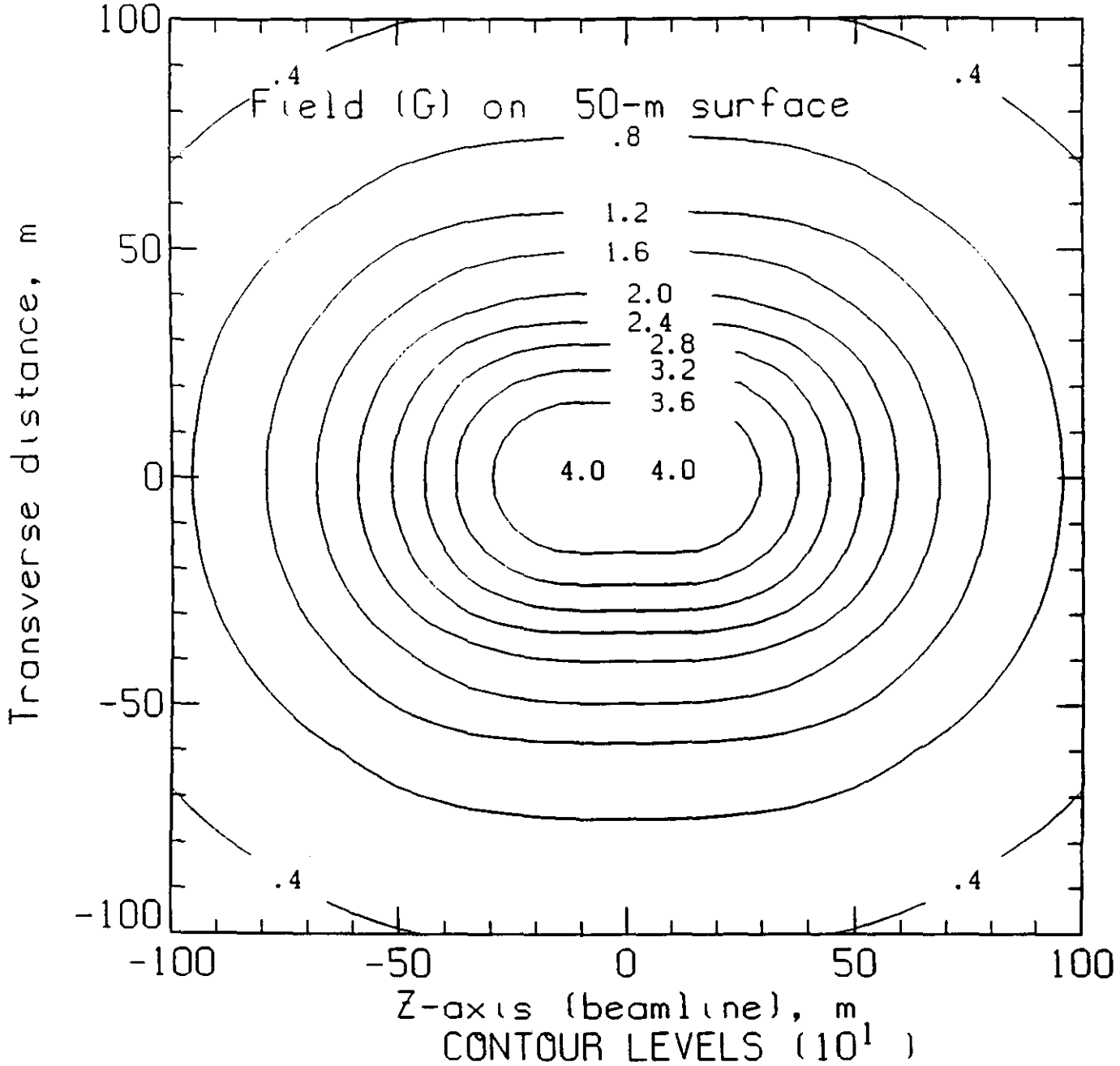

Fig. 7 – Contours of constant flux density at the surface of the earth for the thick pole design for GEM.

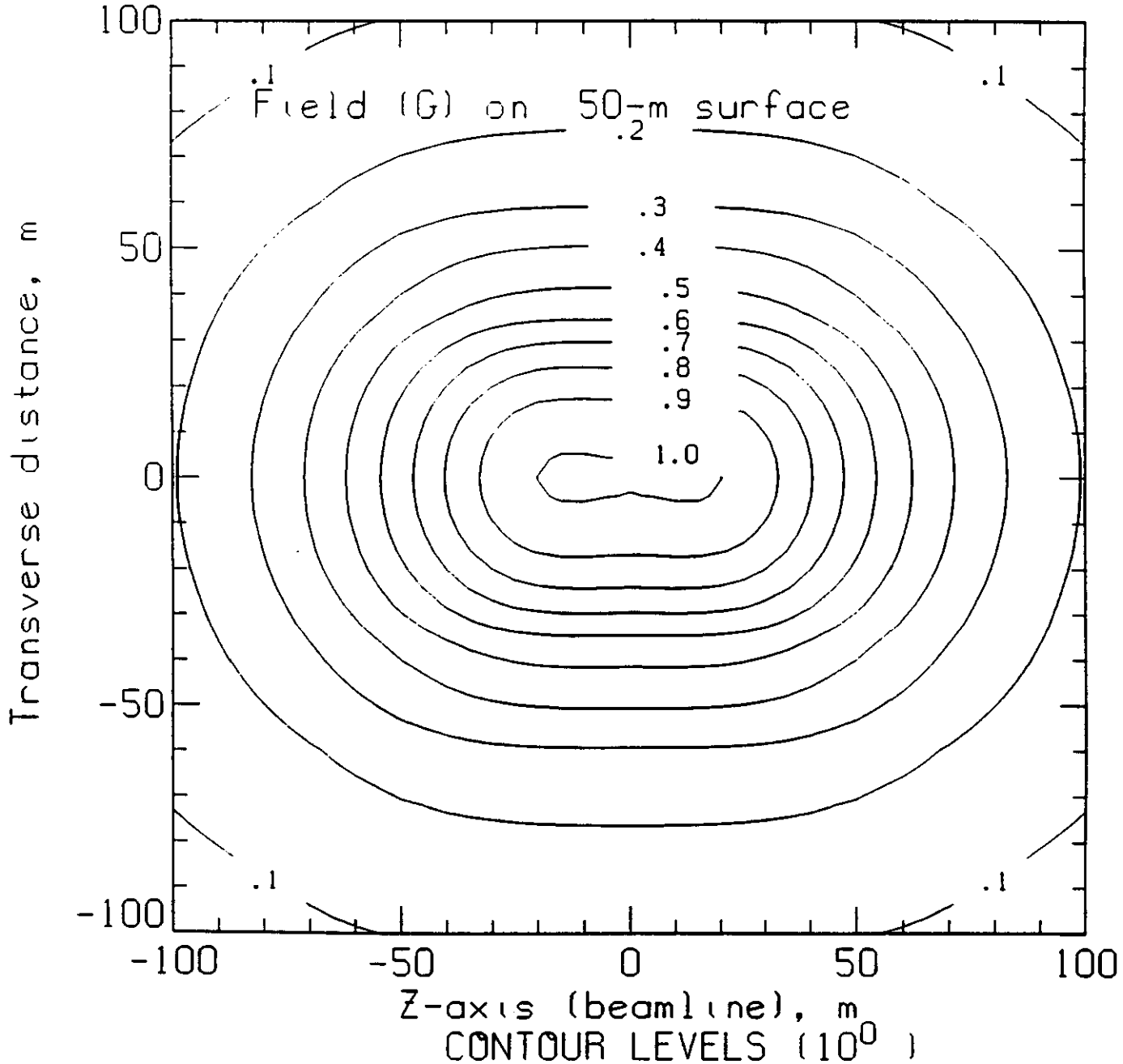

Fig. 8 – Contours of constant flux density at the surface of the earth for the thick pole and 2 m thick iron return frame design for GEM.

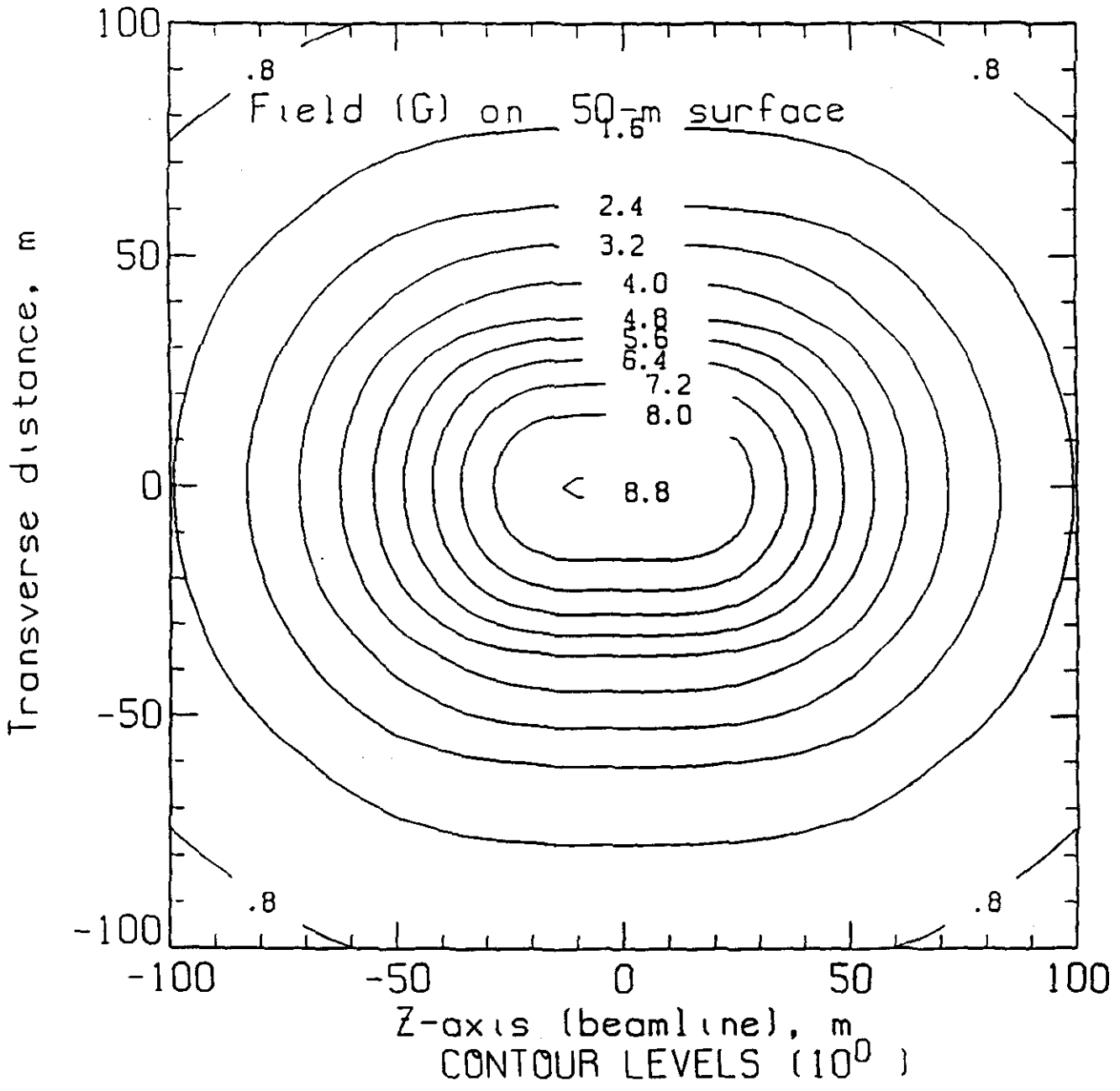

Fig. 9 – Contours of constant flux density at the surface of the earth for the thick pole and 1.3 m thick iron return frame design for GEM.

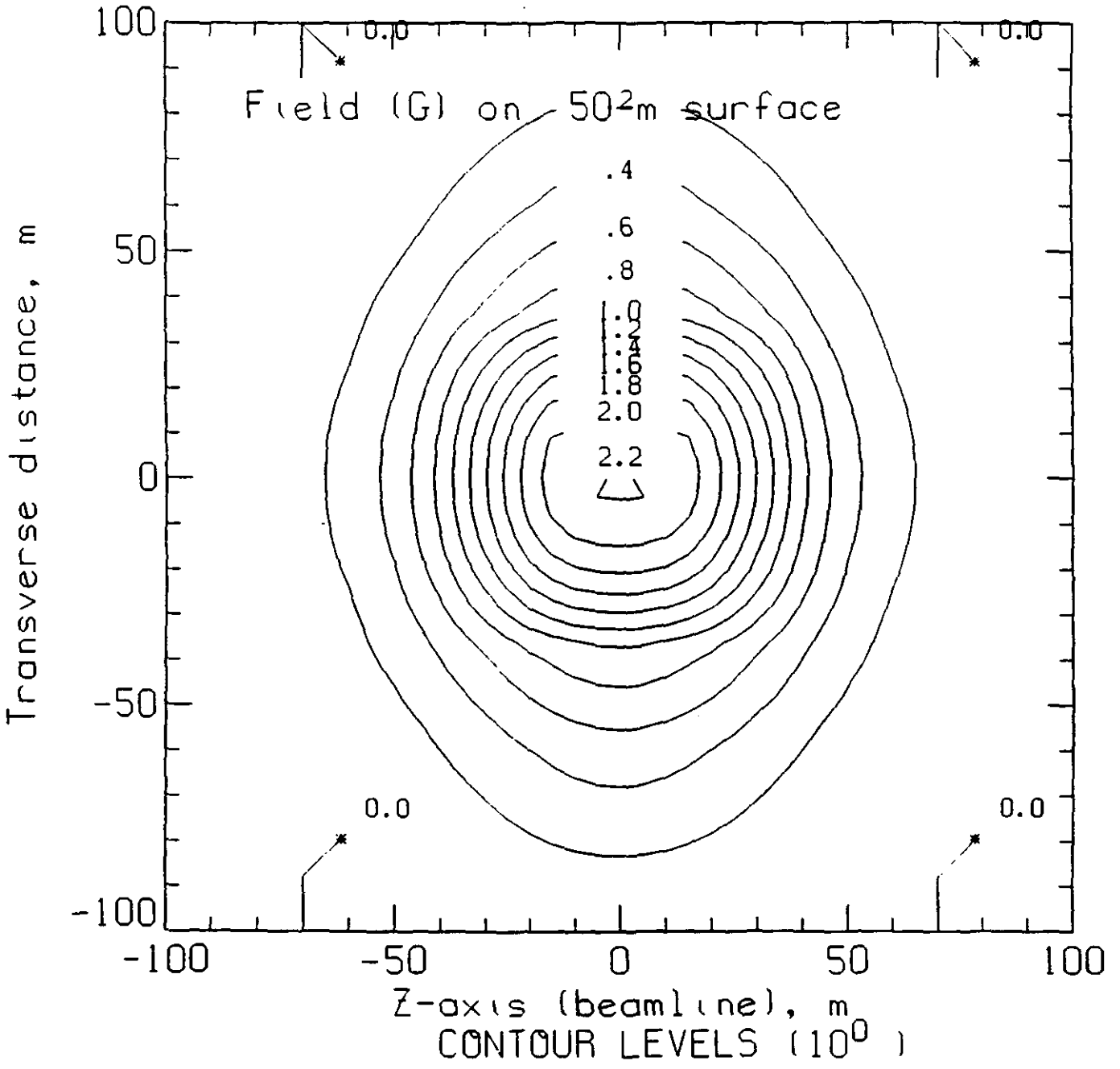

Fig. 10 – Contours of constant flux density at the surface of the earth for the thin pole and double solenoid design for GEM.

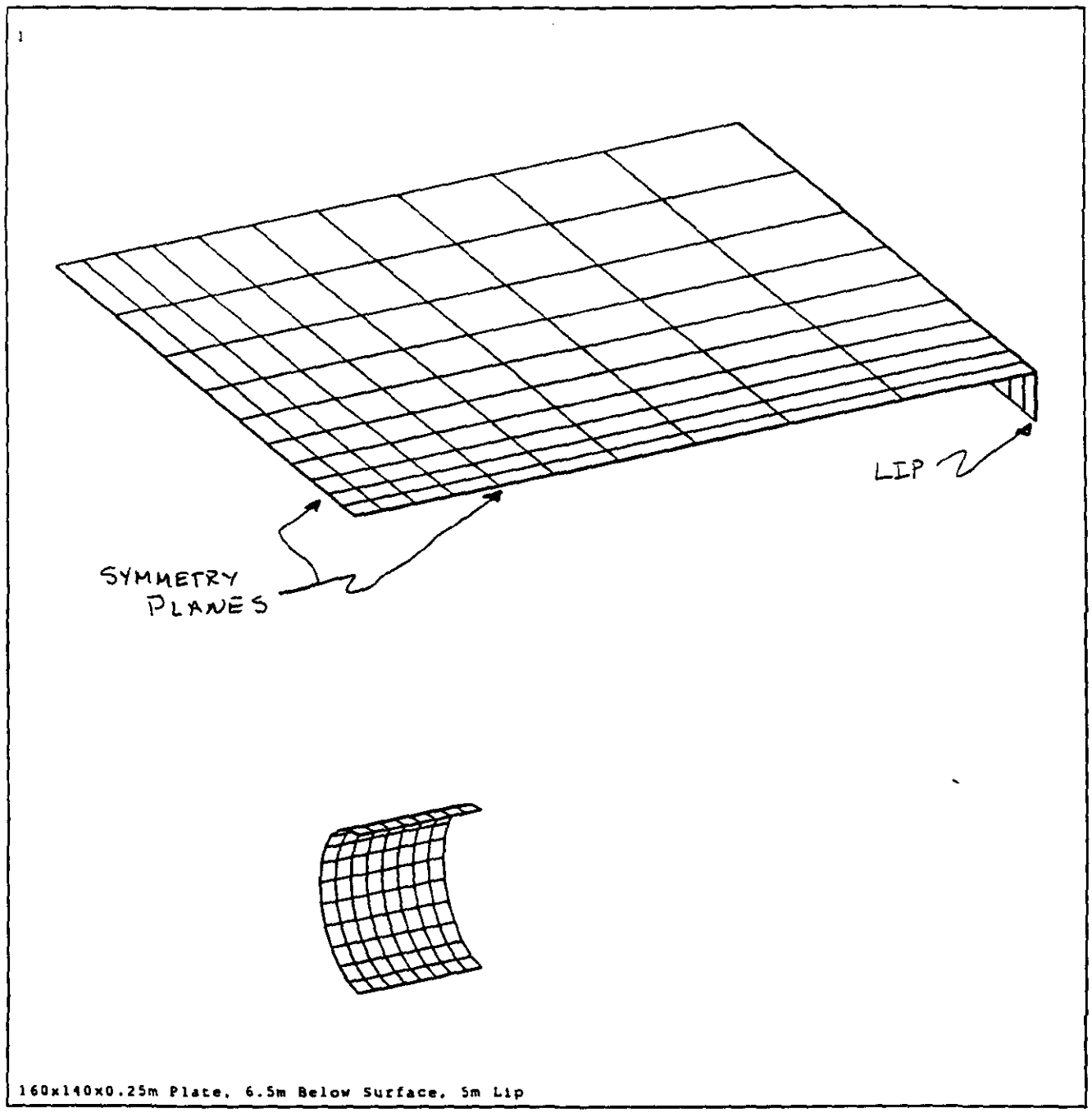

Fig. 11 – Surface plate geometry for shielding surface fields.

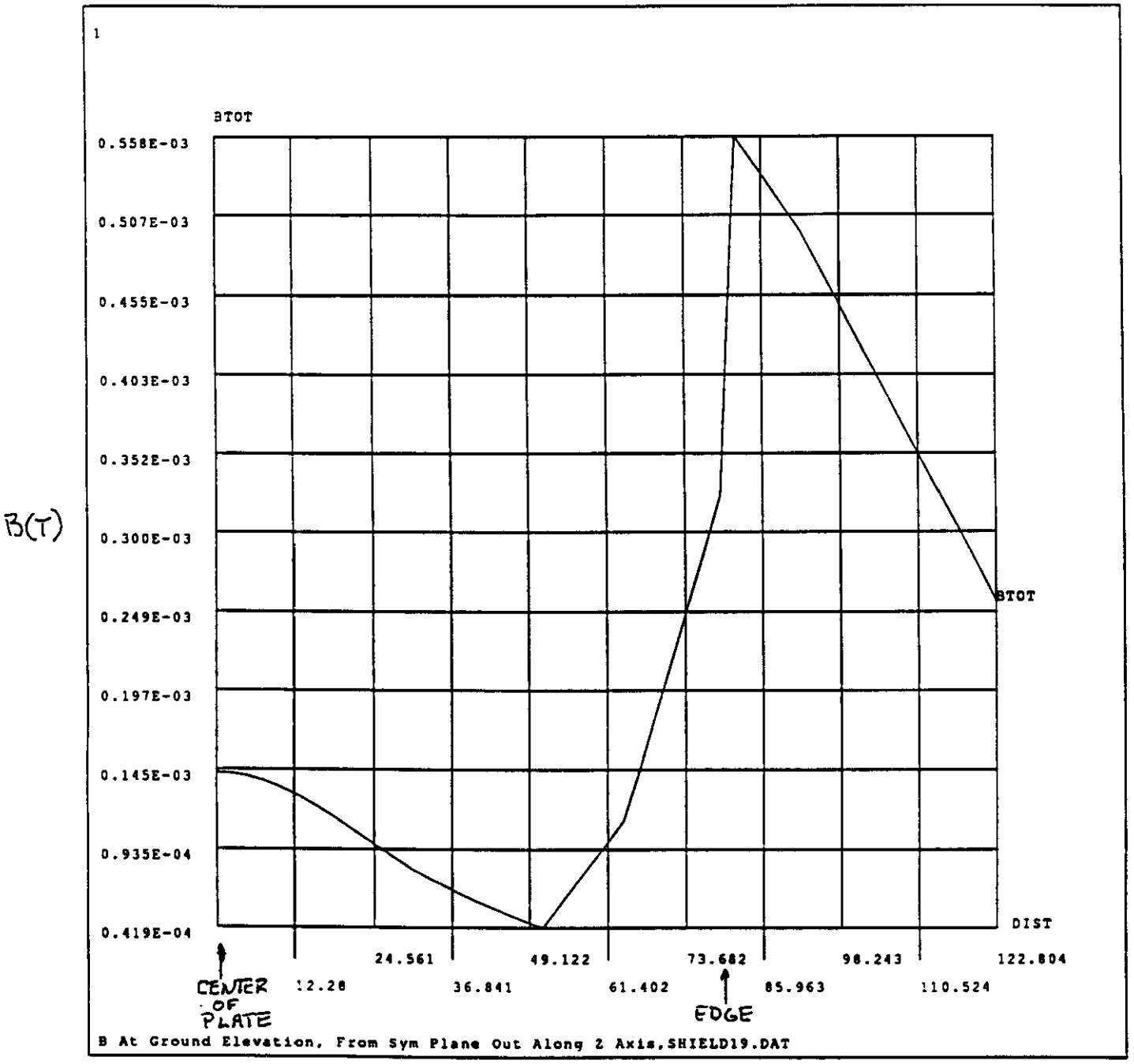

Fig. 12 – Flux density magnitude versus position at the surface.

APPENDIX 3

APPENDIX 3

Superconducting Super Collider Laboratory
2550 Beckleymeade Avenue, Mail Stop 2000
Dallas TX 75237-3946
(214) 708-6168
Fax: (214) 708-6174

Physics Research Division

Memorandum

To: Bob Richardson
From: Warren Kampmeier
Subject: Shielded Valves
Date: November 20, 1991

I have estimated the cost for 20- 1" special solenoid valves at approximately $20,000. The construction of these valves would enable them to operate in the magnetic field anticipated in the GEM hall.

APPENDIX 4

DRAFT

For the electrical components in the detector hall, Warren Kampmeier made a study of the costs associated with dealing with the stray magnetic fields. The SDC hall was used as a model, because more is known about the electrical equipment required for that detector. A field distribution comparable to the GEM unshielded solenoid was assumed. Two methods for dealing with the stray fields were developed: Electrical devices could either be shielded, or oversized to compensate for saturation losses. Of the two, the latter is probably the least expensive, the former is a better solution.

The enclosed spreadsheet assumes that either one or the other method is used for each device depending on cost and effectiveness. For switch-gear and panel boards, the breaker sizes were increased by 20%. The use of larger breakers requires an increase in wire size, thereby leading to an increase in wire cost. Transformers were priced to incorporate special core construction (cast iron) and shielding. Motors in the larger sizes were increased in Hp ratings, and in the smaller sizes double shielded enclosures were added. For lighting fixtures, an added cost was included for remote mounting of high energy discharge lamp ballast transformers.

As shown in the spreadsheet, for a hall comparable to the SDC hall, the stray field would lead to an increase of about $55K for electrical equipment.

POWER DISTRIBUTION ELECTRICAL DEVICE TAKEOFF-Material Only						
Magneticaly Operated Equipment- SDC Hall Area						
Quant	Description	Base Price	Cost	Spcl Price	Cost	Remarks
60Hz ir	input conv					
5	75KVA Trans	1675	8375	2300	11500	
5	200A 208V panels	1440	7200	1440	7200	
2	200A 480V panels	1793	3586	1793	3586	
2	400A 480V panels	1800	3600	1800	3600	6 CBs inc typ
35000	wire			0.06	2100	
2	100Hp motors	3670	7340	4950	9900	
10	25Hp motors	875	8750	956	9560	
Emergency System						
1	200A 208panel	1440	1440	1440	1440	
1	75KVA trans	1675	1675	2300	2300	
1	400A 480V panels	1800	1800	1800	1800	
15000	wire			0.06	900	
Lighting						
1	200A 208panel	1440	1440	1440	1440	
1	75KVA trans	1675	1675	2300	2300	
20	Fixtures Hi Bay	403	8060	903	18060	
20	Fixtures Flour	70	1400	235	4700	
15	Exit	130	1950	340	5100	
HVAC						
3	25 Hp motors	875	2625	956	2868	
1	10Hp butane	363	363	518	518	
22000	wire			0.06	1320	
Special Electronics						
3	400A 480V panels	1800	5400	1800	5400	
9	75KVA Trans	1675	15075	2300	20700	
9	200A 208V panels	1440	12960	1440	12960	
17000	wire			0.06	1020	
Clean Electronics						
3	400A 480V panels	1800	5400	1800	5400	
9	75KVA Trans	1675	15075	2300	20700	
9	200A 208V panels	730	6570	1440	12960	
17000	wire			0.06	1020	
Jacking						
1	Motor Contrl Cntr	9025	9025	9800	9800	
4	100Hp motors	3670	14680	4950	19800	
10000	wire			0.06	600	
	Totals		145464		200552	
	Difference	55088				

APPENDIX 5

APPENDIX 5

Memo to: Peter Marston, Herb Becker, Len Myatt
From P.H.Titus
Oct 25,1991

Subject: Possible source of steel for magnetic shielding

I talked to Gigi (Maybe G.G.) Ross of US Steel in Pittsbugh. She is the sales rep for 'non prime' product. Her phone # is 412 433 4937. (A possible alternate who handles plate sales is Dale Venables,(412) 433 4249)

US Steel produces steel using a continuous casting process. The same mill will produce different product in the same caster. When changing from one product chemistry to another, a transition slab is produced with make-up between the two chemistries. They produce between 1000 and 4000 tons per month of this material. The current price is $150 to $160 per ton, loaded on railcars at the mill. US Steel produces this material at a couple of facilities, The Gary Indiana mill produces slabs 9.11 in. thick, 34 to 96 in. wide, 400 to 480 in. long. At their Birmingham Ala mill 10 in. slabs are produced. This type of product is used for heavy machine bases, and low quality rolled product. They have sold some of the material for magnetic shielding for MRI magnets. Other competitor mills using the continuous casting process produce the same type of material.

Some long term arrangement to take a percentage of this product for use as a shielding material at SSC might be attractive.

APPENDIX 6

LAWRENCE LIVERMORE NATIONAL LABORATORY

6 December, 1991
GEM-LLNL-91-003

MEMORANDUM

To: Ryszard Stroynowski

From: Mike Chaplin, Stewart Shen

Subject: Operational Impact of Fringe Magnetic Field in FENIX

We have recently begun operating the FENIX magnet system at the High-Field Test Facility (HFTF) at LLNL. This superconducting magnet system consists of a pair of coaxial, high-field superconducting (SC) solenoids, arranged so as to produce a net dipole field of 14T at the center. This system is magnetically unshielded, and since it is located near ground level, it produces a large unconfined fringe magnetic field throughout the facility and adjoining areas, as shown in Figure 1. Since we are currently operating this facility, we are quite sensitive to the additional costs associated with the presence of this field. As you observed when you visited HFTF, there are a number of minor one-time costs associated with the magnetic field, such as for local shields around CRT-type devices; it has been suggested that there may also be some recurring costs, due to the impact on the operation of the facility. While we agree that there is certainly some additional cost because of the presence of the magnetic field, for us this cost is so small as to be insignificant.

However, for your use in assessing the potential recurring costs due to the magnetic field surrounding the GEM detector, we provide here a discussion of the nature and magnitude of the operational costs we have actually experienced; where appropriate, we include comments on the extrapolation of our experience to the future GEM conditions. Note that we have not yet accumulated a substantial amount of run time with FENIX; however, our experience with HFTF is quite extensive, including intermittent operation of the HFTF 2m Solenoid System (a facility similar to FENIX, and which produces similar fringe fields) for more than 10 years.

Overall, the most important effect of our fringe magnetic field is that it represents an additional potential hazard to personnel, as described in the LLNL Health and Safety Manual Supplement 26.12 - "Working in Magnetic Fields" (Attachment A). As such, it can lead to additional costs of three general types: 1) additional effort associated with establishing, documenting, and approving appropriate safety precautions; 2) additional effort expended to train personnel to deal with the additional hazard; 3) additional time and effort spent in actually implementing the required additional safety precautions. In addition, the magnetic field could conceivably cause additional costs associated with accelerated breakdown or increased maintenance of equipment which must operate within it. We discuss these four categories separately below.

In the HFTF, DC magnetic fields are considered to be a potential hazard to personnel, and as such, safety precautions must be detailed, documented, and approved, in the form of a Facility Safety Plan (FSP). The FSP for HFTF (Attachment B) deals with all of the potential hazards, which are: high voltage, high current, high internal pressures, cold surfaces, oxygen-deficiency areas, seismic forces, and magnetic fields. Because of the other hazards present, this FSP would have been required even if the magnetic field were not present, but it would then have been roughly 1 page shorter. In considering how this would apply for GEM, note that HFTF does not produce any ionizing radiation; our experience is that the level of safety documentation effort is much higher when this hazard is present, and we therefore expect the incremental cost associated with the magnetic field hazard to be a much smaller fraction of the overall safety documentation effort for GEM. In comparison with ionizing radiation, DC magnetic fields are almost completely benign.

With the establishment of any extra safety precautions comes the requirement to properly implement them, and the first step is personnel training. For FENIX, we require that all workers read and understand the FSP, and that each of them take the courses identified in the FSP (section 8.4, page 25, Attachment B). Note that all these courses (13-14 for each worker) would still be required even if the magnetic field were not present. The additional time required for training is, for us, zero.

Actual implementation of magnetic-field safety precautions does require some time and effort. In our experience, delays have been limited to the time required to post information signs along the 5-gauss line (outside the building), and the time required to sweep the immediate area of loose ferromagnetic materials. For HFTF, these costs are again insignificant. We would expect that this might require more effort for GEM, simply because of the larger areas involved; however, even this cost could be reduced by appropriate design of the protection systems. LLNL is now initiating a medical screening/monitoring program for magnetic-field workers; this program may result in a small cost for yearly health screening for exposed workers.

Finally, the presence of DC magnetic fields might be expected to cause more frequent breakdowns of equipment which must operate nearby. In our experience with HFTF, we have not observed any unusual equipment failures which could be attributed to the presence of the magnetic field. Note, however, that we did perform tests to identify potentially affected equipment (see Attachment C), and we used good practice in locating and shielding these items. We do have a variety of mechanical and electrical equipment which must operate in several-hundred gauss fields, including helium refrigerators, vacuum pumps, etc, and to date we have experienced no difficulties which we can attribute to the magnetic field.

In summary, we have found that the incremental cost due to DC magnetic fields in the HFTF (in the presence of the other hazards) is so small as to be insignificant.

Stewart Shen, Acting Group Leader
SC Magnet Development Group

Mike Chaplin, Facility Manager
HFTF Facility

Attachments:

Attachment A - LLNL Health and Safety Manual Supplement 26.12 - Working in Magnetic Fields
Attachment B - Facility Safety Plan for FENIX (Draft)
Attachment C - (viewgraph on equipment/field tests)